SIAM J. Applied Dynamical Systems
Vol. 20, No. 1, pp. 262–298

Existence of Transonic Solutions in the Stellar Wind Problem with Viscosity and Heat Conduction*

Adam Bauer† and Paul Carter‡

Abstract. The one-fluid stellar wind problem for steady, radial outflow is considered, including effects of heat conduction and viscosity. The associated nondimensionalized equations of conservation of mass, momentum, and energy are singularly perturbed in the large Reynolds number limit, and stellar wind profiles are constructed rigorously in this regime using geometric singular perturbation techniques. Transonic solutions, which accelerate from subsonic to supersonic speeds, are identified as folded saddle canard trajectories lying in the intersection of a subsonic saddle slow manifold and a supersonic repelling slow manifold, returning to subsonic speeds through a viscous layer shock, the location of which is determined by the associated far-field boundary conditions.

Key words. stellar wind, canards, geometric singular perturbation theory

AMS subject classifications. 34E15, 34E17, 76H05, 85A05

DOI. 10.1137/20M1314240

1. Introduction.

A wide body of literature exists on the study of spherically symmetric, steady flow in relation to the stellar wind and accretion problems in astrophysical gas dynamics. These problems concern the outflow and inflow of matter from a massive body, such as a star, under the influence of the body's gravity. This work concerns transonic outflows of matter being ejected from the surface of a star (referred to herein as stellar wind), in which gas accelerates from subsonic to supersonic speeds at some critical radius, before returning to subsonic speeds in the far field. Since Parker's formulation [27], there have been numerous studies of one-fluid models of stellar wind [1, 2, 11, 12, 21, 26, 33, 34] in which numerical and/or asymptotic methods have been employed in analyzing a variety of physically relevant solutions, including those which remain at subsonic speeds for the entire domain, as well as transonic solutions. When the effects of heat conduction and viscosity are neglected, the transonic solutions pass through a singularity, called the sonic point, at which the transition from subsonic to supersonic flow is possible [11]. However, the inclusion of heat conduction and viscosity introduces a regularizing effect which removes the singularity and allows for smooth transonic solutions near the sonic point.

In the small viscosity (large Reynolds number) limit, the challenge comes from the fact that the problem is singularly perturbed, and our aim is to analyze the existence of such transonic

*Received by the editors January 21, 2020; accepted for publication (in revised form) by M. Beck November 23, 2020; published electronically February 18, 2021.
https://doi.org/10.1137/20M1314240
Funding: This work was supported by NSF grant DMS-1815315.
†Department of Physics, University of Illinois Urbana-Champaign, Urbana, IL 61820 USA (adammb4@illinois.edu).
‡School of Mathematics, University of Minnesota, Twin Cities, MN 55455 USA (pcarter@umn.edu).

stellar wind solutions rigorously in the context of geometric singular perturbation theory; these methods allow for the construction of smooth solutions by considering the underlying geometry of the equations on different spatial scales and piecing together this information to build solutions of the full problem. In this context, transonic solutions arise as *canard* trajectories [37], which manifest as intersections of repelling and attracting slow manifolds. Canards are frequently important in understanding the dynamics in singularly perturbed dynamical systems and arise naturally in applications in mathematical biology, physiology, and physics. In the context of transonic flows, canards have been shown to organize the dynamics of the hydrodynamic escape problem [13] and the dynamics of flow through a nozzle [14, 16, 17, 24]; in particular, sub-to-supersonic canard trajectories analogous to those considered here have been analyzed in [16] in relation to flow through contracting-expanding nozzles.

In the context of stellar winds, prior work [4] demonstrated the existence of transonic solutions in a related setting; these solutions arise as canard trajectories lying in the intersection of attracting and repelling branches of a two-dimensional slow manifold, accompanied by a viscous shock to return to subsonic speeds in the far field. However, in [4], viscosity was assumed constant, and the effects of heat conduction were neglected in favor of a simplified assumption of isentropic (constant entropy) flow. It should be noted that this assumption is, at best, a rough approximation in this context, given that shocks are associated with a change in entropy. Additionally, one expects that the effect of thermal diffusivity is of greater magnitude than that of viscosity in the context of stellar wind, and therefore a treatment of the stellar wind phenomenon should include both effects. In this spirit, the goal of the current work is to analyze stellar winds, relaxing the assumption of isentropic flow, retaining heat conduction, and allowing the viscosity to depend on temperature. Ultimately, the effect on the analysis is that the resulting equations for stationary solutions are of higher order; this introduces some technical challenges in the construction of canard orbits which satisfy the far-field boundary conditions.

We consider a star of mass M at rest in an infinite gas cloud with an ambient density ρ_∞, thermodynamic pressure p_∞, and temperature T_∞ at infinity. In the entire domain, we assume that the pressure, p, is related to the density ρ and temperature T of the system by the ideal gas law, i.e.,

$$p = p(\rho, T) = \rho R T, \tag{1.1}$$

where $R > 0$ is the specific gas constant. We consider spherically symmetric flow under the force of gravity only, with force in the radial component

$$F = -\rho \frac{GM}{r^2} \hat{r}, \tag{1.2}$$

where $G > 0$ is the gravitational constant and $r \geq 0$ is the radial distance. The dynamics for the one-fluid model of the stellar wind are then governed by the compressible, viscous Navier–Stokes equations describing conservation of mass, momentum, and energy

$$
\begin{aligned}
&\frac{\partial \rho}{\partial \tau} + \frac{1}{r^2}\frac{\partial}{\partial r}\left(\rho r^2 u\right) = 0,\\
&\frac{\partial}{\partial \tau}\left(\rho u\right) + \frac{1}{r^2}\frac{\partial}{\partial r}\left(\rho r^2 u^2\right) + \frac{\partial p}{\partial r} + \frac{GM\rho}{r^2}\\
&\quad = \frac{4}{3}\left(\eta\left(\frac{\partial}{\partial r}\left(\frac{1}{r^2}\frac{\partial}{\partial r}\left(r^2 u\right)\right) + \frac{\partial \eta}{\partial r}\left(\frac{\partial u}{\partial r} - \frac{u}{r}\right)\right)\right),\\
&\frac{\partial}{\partial \tau}\left(\frac{1}{2}\rho u^2 + \rho e\right) + \frac{1}{r^2}\frac{\partial}{\partial r}\left(r^2\left(\frac{1}{2}\rho u^3 + \rho u e + p u\right)\right)\\
&\quad = \frac{1}{r^2}\frac{\partial}{\partial r}\left(r^2\left(\zeta\frac{\partial T}{\partial r} + \frac{4}{3}\eta u\left(\frac{\partial u}{\partial r} - \frac{u}{r}\right)\right)\right) - \rho u\frac{GM}{r^2},
\end{aligned}
\tag{1.3}
$$

where τ denotes time, $u \in \mathbb{R}$ is the radial velocity, $e = \frac{p}{\rho(\gamma-1)}$ is the internal energy, and $1 < \gamma < \frac{5}{3}$ is the ratio of specific heats [1]. Here $u > 0$ corresponds to outflow (stellar wind, i.e., away from the star) and $u < 0$ corresponds to inflow (accretion, i.e., toward the star). While we focus on the outflow problem in this paper, the techniques could be adjusted in a straightforward fashion to apply to the corresponding inflow problem as well. The flow is considered to be subsonic if $|u| < c$ and supersonic if $|u| > c$, where

$$
c := \left(\frac{\gamma\rho}{p}\right)^{\frac{1}{2}} = \sqrt{\gamma RT} > 0 \tag{1.4}
$$

is the adiabatic speed of sound. We include the effects of both temperature-dependent viscosity and heat conduction, though under the assumption that viscosity and thermal diffusivity are small; that is, we consider the regime of large Reynolds number and large Péclet number. We further assume that thermal diffusivity dominates viscosity so that the corresponding Prandtl number, equivalent to the ratio of the Péclet number and Reynolds number, is small. We further assume that the viscosity, $\eta = \eta(T)$, and the thermal conductivity, $\zeta = \zeta(T)$, are both increasing functions of temperature. The specific dependence of $\eta(T)$ and $\zeta(T)$ will be discussed later in this paper, though our analysis is valid in particular for functions $\eta(T), \zeta(T) \propto T^{\omega}, \omega > 1$.

In this setting, the model (1.3) admits families of solutions which are subsonic on the entire domain, as well as transonic solutions which accelerate to supersonic speeds through the so-called sonic point and decelerate to subsonic speeds in the far-field via a viscous shock, the location of which is determined by the far-field boundary conditions. Analogously to [4], these transonic solutions appear as canards, though due to the addition of the full energy equation in (1.3), the associated equations are of higher order, and thus the state space dimension is larger. The canard trajectories lie on the intersection of a saddle-type slow manifold and a normally repelling slow manifold in a four-dimensional singularly perturbed dynamical system (this is in contrast to those seen in, e.g., [9], in which the canard orbits lie on the intersection of attracting and saddle-type slow manifolds), and the transition to subsonic speeds in the far-field occurs through a fast heteroclinic orbit in the two-dimensional layer problem. The exact choice of heteroclinic orbit traversed is determined by boundary manifolds at infinity which select the correct far-field boundary conditions; these are obtained through a compactification procedure.

The remainder of this paper is outlined as follows. In section 2, we describe the setup and statement of our main existence results, and we nondimensionalize the equations which, in the large Reynolds number limit, results in a singular perturbed dynamical system in the radial coordinate. The singular slow and fast limits of this system are analyzed in section 3 in the context of geometric singular perturbation theory, and we construct families of singular solution orbits. In section 4, we show that these singular orbits perturb smoothly to steady stellar wind solutions of (1.3) satisfying appropriate boundary conditions, and we conclude with a brief discussion in section 5.

2. Setup.

We search for steady stellar wind profiles, for which (1.3) reduces to the following system of ordinary differential equations in the radial coordinate r:

$$\frac{1}{r^2}\frac{\mathrm{d}}{\mathrm{d}r}\left(\rho r^2 u\right) = 0, \tag{2.1}$$

$$\frac{1}{r^2}\frac{\mathrm{d}}{\mathrm{d}r}\left(\rho r^2 u^2\right) + \frac{\mathrm{d}p}{\mathrm{d}r} + \frac{GM\rho}{r^2} = \frac{4}{3}\left(\eta(T)\left(\frac{\mathrm{d}}{\mathrm{d}r}\left(\frac{1}{r^2}\frac{\mathrm{d}}{\mathrm{d}r}\left(r^2 u\right)\right)\right) + \frac{\mathrm{d}\eta(T)}{\mathrm{d}r}\left(\frac{\mathrm{d}u}{\mathrm{d}r} - \frac{u}{r}\right)\right), \tag{2.2}$$

$$\frac{1}{r^2}\frac{\mathrm{d}}{\mathrm{d}r}\left(r^2\left(\frac{1}{2}\rho u^3 + \rho u e + p u\right)\right) = \frac{1}{r^2}\frac{\mathrm{d}}{\mathrm{d}r}\left(r^2\left(\zeta\frac{\mathrm{d}T}{\mathrm{d}r} + \frac{4}{3}\eta(T)u\left(\frac{\mathrm{d}u}{\mathrm{d}r} - \frac{u}{r}\right)\right)\right) - \rho u\frac{GM}{r^2}. \tag{2.3}$$

In this section, we prepare these equations for the forthcoming analysis. In section 2.1, we reduce (2.1)–(2.3) to a first order system, and we state our main results concerning transonic stellar wind solutions in section 2.2. In section 2.3, we nondimensionalize the system, obtaining a singularly perturbed dynamical system which will be analyzed using geometric singular perturbation techniques in section 3.

2.1. Preparation of equations.

The equation describing conservation of mass (2.1) can be integrated immediately, so that $\rho r^2 u = K$ with constant *mass flux* $K > 0$ for the outflow problem $u > 0$. We can therefore express the density ρ in terms of the radial distance r, and velocity u as

$$\rho(r,u) = \frac{K}{r^2 u} > 0. \tag{2.4}$$

Using the ideal gas law (1.1), the pressure, $p(\rho,T)$, can be represented as a function of r, u, and the temperature T, given by

$$p(\rho(r,u),T) = \rho(r,u)RT = \frac{KRT}{r^2 u} > 0. \tag{2.5}$$

We now consider the equation of momentum conservation (2.2), which after rearranging becomes

$$\frac{\mathrm{d}}{\mathrm{d}r}(\rho u^2 + p) - \frac{4}{3}\left(\eta(T)\left(\frac{\mathrm{d}}{\mathrm{d}r}\left(\frac{1}{r^2}\frac{\mathrm{d}}{\mathrm{d}r}(r^2 u)\right)\right) + \frac{\mathrm{d}\eta(T)}{\mathrm{d}r}\left(\frac{\mathrm{d}u}{\mathrm{d}r} - \frac{u}{r}\right)\right) = -\frac{2\rho u^2}{r} - \frac{GM\rho}{r^2},$$

from which we obtain

$$\frac{\mathrm{d}}{\mathrm{d}r}\left(\rho u^2 + p - \frac{4}{3}\eta(T)\frac{\mathrm{d}u}{\mathrm{d}r} - \frac{8}{3}\eta(T)\frac{u}{r}\right) = -\frac{2\rho u^2}{r} - \frac{GM\rho}{r^2} - \frac{4u}{r}\frac{\mathrm{d}\eta(T)}{\mathrm{d}r}.$$

We therefore define an auxiliary variable with physical dimensions of pressure

$$m := \rho u^2 + p - \frac{4}{3}\eta(T)\frac{\mathrm{d}u}{\mathrm{d}r} - \frac{8}{3}\eta(T)\frac{u}{r}, \tag{2.6}$$

which leads to the system

$$\begin{aligned} \frac{\mathrm{d}m}{\mathrm{d}r} &= -\frac{2\rho u^2}{r} - \frac{GM\rho}{r^2} - \frac{4u}{r}\frac{\mathrm{d}\eta(T)}{\mathrm{d}r}, \\ \eta(T)\frac{\mathrm{d}u}{\mathrm{d}r} &= \frac{3}{4}(\rho u^2 + p - m) - \frac{2u}{r}\eta(T). \end{aligned} \tag{2.7}$$

Finally we consider the equation of energy conservation (2.3), which can be integrated once using (2.4) and rearranged to yield

$$\frac{1}{2}\rho u^3 + \frac{\gamma p u}{\gamma - 1} = \frac{EK}{r^2} + \zeta(T)\frac{\mathrm{d}T}{\mathrm{d}r} + \frac{4}{3}\eta(T)u\left(\frac{\mathrm{d}u}{\mathrm{d}r} - \frac{u}{r}\right) + \frac{GM\rho u}{r}, \tag{2.8}$$

where E is the specific energy (energy per unit mass) of the fluid, assumed to be positive. Substituting (2.7) for $\eta(T)\frac{\mathrm{d}u}{\mathrm{d}r}$ and simplifying, we obtain

$$\zeta(T)\frac{\mathrm{d}T}{\mathrm{d}r} = um + \frac{4\eta(T)u^2}{r} + \frac{pu}{\gamma - 1} - \frac{GM\rho u}{r} - \frac{EK}{r^2} - \frac{1}{2}\rho u^3. \tag{2.9}$$

Combining the results from (2.7) and (2.9), and using the expressions (2.4) and (2.5) for the density and pressure, respectively, we obtain the nonautonomous system of ODEs in r for (m, u, T)

$$\begin{aligned} \frac{\mathrm{d}m}{\mathrm{d}r} &= -\frac{2Ku}{r^3} - \frac{GMK}{r^4 u} - \frac{4u}{r}\frac{\mathrm{d}\eta(T)}{\mathrm{d}r}, \\ \eta(T)\frac{\mathrm{d}u}{\mathrm{d}r} &= \frac{3}{4}\left(\frac{Ku}{r^2} + \frac{KRT}{ur^2} - m\right) - \frac{2u}{r}\eta(T), \\ \zeta(T)\frac{\mathrm{d}T}{\mathrm{d}r} &= um + \frac{4\eta(T)u^2}{r} + \frac{1}{\gamma - 1}\frac{KRT}{r^2} - \frac{GMKu}{r^3} - \frac{EK}{r^2} - \frac{1}{2}\frac{Ku^2}{r^2}, \end{aligned} \tag{2.10}$$

which we consider on the interval $r \in (r_0, \infty)$ where r_0 denotes a nonzero reference radial distance (for instance, the stellar surface).

2.2. Statement of main result: Stellar wind solutions. In this section, we state our main existence result concerning transonic stellar winds. We define c to be the speed of sound

$$c = \sqrt{\gamma RT}. \tag{2.11}$$

A solution to (2.10) is then *subsonic* whenever $|u(r)| < c$ and *supersonic* whenever $|u(r)| > c$. A *transonic* solution $(m, u, T) = (m(r), u(r), T(r))$ on the interval $r \in (r_0, \infty)$ to (2.10) satisfies the following:

(i) The velocity profile $u(r)$ is subsonic at the inner boundary $r = r_0$ and asymptotically subsonic as $r \to \infty$.

(ii) $u(r)$ is supersonic for some interval I, where $I \subset (r_0, \infty)$ is a bounded interval.

Given fixed mass flux $K > 0$, specific energy $E > 0$, and stellar radius r_0, the system (2.10) supports steady transonic stellar wind solutions under certain constraints on the asymptotic physical boundary conditions; otherwise only subsonic solutions are supported. We have the following.

Theorem 2.1. *Consider* (2.10) *for any fixed* $\gamma \in (1, 5/3)$ *and sufficiently small Prandtl number* $\theta > 0$. *There exists* k_∞ *such that for any fixed asymptotic temperature* $T_\infty \in (0, \infty)$ *and asymptotic pressure* $p_\infty \in (0, \infty)$, *the following holds*:

(i) *If* $p_\infty^2 > k_\infty T_\infty$ *or* $r_0 > \frac{GM(5-3\gamma)}{4E(\gamma-1)}$, *then for any sufficiently large Reynolds number* $\mathrm{Re} \gg 1$, *there exists a pressure,* $p(r_0) = p_0$, *and temperature,* $T(r_0) = T_0$, *at the stellar surface* $r = r_0$ *that supports a steady subsonic solution for* $r \in (r_0, \infty)$ *satisfying* $(m(r), T(r)) \to (p_\infty, T_\infty)$ *as* $r \to \infty$.

(ii) *If* $p_\infty^2 < k_\infty T_\infty$ *and* $r_0 < \frac{GM(5-3\gamma)}{4E(\gamma-1)}$, *then for any sufficiently large Reynolds number* $\mathrm{Re} \gg 1$, *there exists a pressure,* $p(r_0) = p_0$, *and temperature,* $T(r_0) = T_0$, *at the stellar surface* $r = r_0$ *that supports a steady transonic stellar wind solution for* $r \in (r_0, \infty)$ *satisfying* $(m(r), T(r)) \to (p_\infty, T_\infty)$ *as* $r \to \infty$.

Remark 2.2. We briefly comment on the two conditions in Theorem 2.1 which determine whether transonic stellar wind solutions are supported for the given physical boundary conditions. The first condition relates the asymptotic pressure and temperature which, through the ideal gas law, can also be related to the corresponding asymptotic density. We find that if the asymptotic pressure is too large relative to the temperature, only subsonic solutions are supported, while lower relative values of the pressure can support transonic winds. We will show in section 4 that the constant k_∞ can be determined explicitly as

$$k_\infty = \frac{K^2 R}{\gamma} \left(\frac{2(\gamma-1)E}{GM} \right)^4 (10 - 6\gamma)^{\frac{5-3\gamma}{\gamma-1}}.$$

The second condition concerns the stellar radius r_0. We will show that winds which are subsonic at the stellar surface can only accelerate to supersonic speeds by crossing the corresponding sonic point, which occurs at the critical radius $r = \frac{GM(5-3\gamma)}{4E(\gamma-1)}$. Hence if the stellar radius extends further than this critical radius, no transonic winds are supported.

Remark 2.3. It can be determined immediately from the critical radius $r = \frac{GM(5-3\gamma)}{4E(\gamma-1)}$ of the sonic point that transonic solutions exist only in the physical regime $\gamma \in (1, 5/3)$, as the sonic point occurs at $r = 0$ (resp., $r = \infty$) in the limit $\gamma \to 5/3$ (resp., $\gamma \to 1$). Furthermore, we will show in section 4.4 that for values of $\gamma \in (3/2, 5/3)$, while transonic solutions can exist, the physical velocity decelerates when crossing the sonic point, due to the fact that c decreases rapidly through the sonic point. We therefore determine that only for values of $\gamma \in (1, 3/2)$ does the system admit transonic solutions which accelerate through the sonic point [6, 13, 38].

2.3. Dimensional analysis. We first transform the system (2.10) to dimensionless variables by introducing reference scales for the variables (r, m, u, T). As a reference velocity, we choose the speed of sound c, as defined in (2.11), and we set

$$u = cv, \tag{2.12}$$

where v is the local Mach number. Note that this rescaling depends on the spatial coordinate r through the temperature T. We then introduce constant reference scalings (to be determined) for the remaining variables as

$$r = k_r s, \qquad m = k_m n, \qquad T = k_T t, \tag{2.13}$$

where $k_r, k_m, k_T > 0$. Additionally, the viscosity and thermal conductivity are assumed to scale as $\eta(T), \zeta(T) \propto T^\omega$ with $\omega = 5/2$ [1, 5, 7, 11], and we therefore set

$$\eta(T) = \eta_0 \bar{\eta}(t), \qquad \zeta(T) = \zeta_0 \bar{\zeta}(t), \tag{2.14}$$

where

$$\bar{\eta}(t) = \bar{\zeta}(t) = t^{5/2}. \tag{2.15}$$

Here the quantities η_0 and ζ_0 contain all the dimensional information about the viscosity and the thermal conductivity, respectively, while $\bar{\eta}(t)$ and $\bar{\zeta}(t)$ capture how the viscosity and thermal conductivity scale in t. While we fix the exponent $\omega = 5/2$ for clarity of presentation, we remark that the following analysis could be modified to hold for any $\omega > 1$.

Substituting these scalings into (2.10), and using the relations

$$\begin{aligned} \frac{\mathrm{d}\eta(T)}{\mathrm{d}r} &= \frac{\eta_0}{k_r}\bar{\eta}'(t)\frac{\mathrm{d}t}{\mathrm{d}s}, \\ \frac{\mathrm{d}(cv)}{\mathrm{d}r} &= \frac{\sqrt{\gamma R k_T}}{k_r}\left(\frac{v}{2\sqrt{t}}\frac{\mathrm{d}t}{\mathrm{d}s} + \sqrt{t}\frac{\mathrm{d}v}{\mathrm{d}s}\right), \end{aligned} \tag{2.16}$$

we arrive at the nondimensionalized system

$$\begin{aligned} \frac{\mathrm{d}n}{\mathrm{d}s} &= -\frac{2K\sqrt{\gamma R k_T}}{k_m k_r^2}\frac{v\sqrt{t}}{s^3} - \frac{GMK}{k_r^3\sqrt{\gamma R k_T}}\frac{1}{v\sqrt{t}s^4} - \frac{4\eta_0\sqrt{\gamma R k_T}}{k_r}\frac{v\sqrt{t}}{s}\bar{\eta}'(t)\frac{\mathrm{d}t}{\mathrm{d}s}, \\ \frac{\mathrm{d}v}{\mathrm{d}s} &= \frac{3}{4\bar{\eta}(t)}\left(\frac{K}{\eta_0 k_r}\frac{v}{s^2} + \frac{K}{\gamma\eta_0 k_r}\frac{1}{vs^2} - \frac{k_m k_r}{\eta_0\sqrt{\gamma R k_T}}\frac{n}{\sqrt{t}}\right) - \frac{2v}{s} - \frac{1}{2}\frac{v}{t}\frac{\mathrm{d}t}{\mathrm{d}s}, \\ \frac{\mathrm{d}t}{\mathrm{d}s} &= \frac{1}{\bar{\zeta}(t)}\left(\sqrt{\frac{\gamma R}{k_T}}\frac{k_r k_m}{\zeta_0}v\sqrt{t}n - \frac{\gamma K R}{2\zeta_0 k_r}\frac{v^2 t}{s^2} - \frac{GMK}{\zeta_0 k_r^2 k_T}\frac{1}{s^3} + \frac{4\gamma\eta_0 R}{\zeta_0}\frac{v^2 t}{s}\bar{\eta}(t)\right. \\ &\qquad \left. + \frac{KR}{(\gamma-1)\zeta_0 k_r}\frac{t}{s^2} - \frac{EK}{\zeta_0 k_r k_T}\frac{1}{s^2}\right). \end{aligned} \tag{2.17}$$

We now introduce the following dimensionless quantities:

$$\frac{1}{\varepsilon_R} := \frac{K}{\eta_0 k_r}, \qquad \frac{1}{\varepsilon_P} := \frac{K\gamma R}{\zeta_0 k_r(\gamma-1)}, \tag{2.18}$$

where ε_R is the inverse Reynolds number and ε_P is the inverse Péclet number [1]. We consider the regime in which the Reynolds number and the Péclet number are both large, and thus

we have that $0 < \varepsilon_R, \varepsilon_P \ll 1$ [11]. We also introduce the Prandtl number as the ratio of the Péclet and Reynolds numbers

$$\theta := \frac{\eta_0 \gamma R}{\zeta_0(\gamma - 1)} = \frac{\varepsilon_R}{\varepsilon_P}. \tag{2.19}$$

In the context of stellar winds, it is reasonable to expect that thermal diffusivity dominates effects of viscosity, and hence the Prandtl number is assumed small, with estimates on the order of 10^{-2} [21, 36, 40]. Therefore, in our analysis we consider the regime $0 < \varepsilon_R \ll \theta \ll 1$, and we will use the Prandtl number to eliminate the Péclet number from the analysis; we therefore remove the subscript from ε_R and denote $\varepsilon := \varepsilon_R$.

We further choose the reference scalings

$$k_r := \frac{GM}{E\alpha}, \qquad k_m := \frac{KE^2\alpha^2}{G^2M^2}\sqrt{\frac{E}{\gamma - 1}}, \qquad k_T := \frac{E(\gamma - 1)}{\gamma R}, \tag{2.20}$$

for some $\alpha > 0$ to be determined. With these scalings, after some rearranging, we arrive at the nonautonomous system

$$\begin{aligned}
\frac{\mathrm{d}n}{\mathrm{d}s} &= -2(\gamma - 1)\frac{v\sqrt{t}}{s^3} - \frac{\alpha}{v\sqrt{t}s^4} - 4(\gamma - 1)\frac{v\sqrt{t}}{s}\bar{\eta}'(t)\varphi(s, n, v, t, \epsilon), \\
\varepsilon\frac{\mathrm{d}v}{\mathrm{d}s} &= \frac{3}{4\bar{\eta}(t)}\left(\frac{v}{s^2} + \frac{1}{\gamma}\frac{1}{vs^2} - \frac{1}{\gamma - 1}\frac{n}{\sqrt{t}}\right) - 2\varepsilon\frac{v}{s} - \frac{1}{2}\frac{v}{t}\varphi(s, n, v, t, \epsilon), \\
\varepsilon\frac{\mathrm{d}t}{\mathrm{d}s} &= \frac{\theta}{\bar{\zeta}(t)}\left(vn\sqrt{t} - \frac{\gamma - 1}{2}\frac{v^2t}{s^2} - \frac{\alpha}{s^3} + \frac{1}{\gamma}\frac{t}{s^2} - \frac{1}{s^2} + 4\varepsilon(\gamma - 1)\bar{\eta}(t)\frac{v^2t}{s}\right),
\end{aligned} \tag{2.21}$$

where the quantity $\varphi(s, n, v, t, \epsilon)$, which appears in the first two equations, is shorthand for the right-hand side of the third equation for temperature

$$\varphi(s, n, v, t, \epsilon) := \frac{\theta}{\bar{\zeta}(t)}\left(vn\sqrt{t} - \frac{\gamma - 1}{2}\frac{v^2t}{s^2} - \frac{\alpha}{s^3} + \frac{1}{\gamma}\frac{t}{s^2} - \frac{1}{s^2} + 4\varepsilon(\gamma - 1)\bar{\eta}(t)\frac{v^2t}{s}\right). \tag{2.22}$$

3. Slow/fast analysis. We now view the nondimensionalized equations (2.21) as a singularly perturbed dynamical system with small parameter $\varepsilon \ll 1$. The parameter θ will also be taken small in the analysis, but since we assume $\varepsilon \ll \theta \ll 1$, the effect of θ in (2.21) is that of a regular perturbation. We next introduce a dummy variable $y = s$ to make the system autonomous, resulting in the four-dimensional autonomous system

$$\begin{aligned}
\frac{\mathrm{d}s}{\mathrm{d}y} &= g_1(s, n, v, t, \varepsilon) := 1, \\
\frac{\mathrm{d}n}{\mathrm{d}y} &= g_2(s, n, v, t, \varepsilon) := -2(\gamma - 1)\frac{v\sqrt{t}}{s^3} - \frac{\alpha}{v\sqrt{t}s^4} - 4(\gamma - 1)\frac{v\sqrt{t}}{s}\bar{\eta}'(t)\varphi(s, n, v, t), \\
\varepsilon\frac{\mathrm{d}v}{\mathrm{d}y} &= f_1(s, n, v, t, \varepsilon) := \frac{3}{4\bar{\eta}(t)}\left(\frac{v}{s^2} + \frac{1}{\gamma}\frac{1}{vs^2} - \frac{1}{\gamma - 1}\frac{n}{\sqrt{t}}\right) - 2\varepsilon\frac{v}{s} - \frac{1}{2}\frac{v}{t}\varphi(s, n, v, t, \epsilon), \\
\varepsilon\frac{\mathrm{d}t}{\mathrm{d}y} &= f_2(s, n, v, t, \varepsilon) := \frac{\theta}{\bar{\zeta}(t)}\left(vn\sqrt{t} - \frac{\gamma - 1}{2}\frac{v^2t}{s^2} - \frac{\alpha}{s^3} + \frac{1}{\gamma}\frac{t}{s^2} - \frac{1}{s^2} + 4\varepsilon(\gamma - 1)\bar{\eta}(t)\frac{v^2t}{s}\right).
\end{aligned} \tag{3.1}$$

The system (3.1) can now be viewed as a "slow-fast" dynamical system with two "slow" variables (s, n) and two "fast" variables (v, t), and timescale separation parameter $0 < \varepsilon \ll 1$. We refer to (3.1), which evolves on the slow timescale y as the *slow system*. By rescaling the dummy variable $y = \varepsilon z$, we obtain the equivalent system

$$\begin{aligned} \frac{\mathrm{d}s}{\mathrm{d}z} &= \varepsilon g_1(s, n, v, t, \varepsilon), \\ \frac{\mathrm{d}n}{\mathrm{d}z} &= \varepsilon g_2(s, n, v, t, \varepsilon), \\ \frac{\mathrm{d}v}{\mathrm{d}z} &= f_1(s, n, v, t, \varepsilon), \\ \frac{\mathrm{d}t}{\mathrm{d}z} &= f_2(s, n, v, t, \varepsilon) \end{aligned} \tag{3.2}$$

on the fast timescale z, which we refer to as the *fast system*.

3.1. Singular limits. The systems (3.1) and (3.2) are equivalent for any $\varepsilon > 0$. The idea of geometric singular perturbation theory is to infer information about the solutions of the full system for $\varepsilon > 0$ by separately analyzing the singular limiting systems obtained by taking the limit $\varepsilon \to 0$ in each of (3.1) and (3.2).

Setting $\varepsilon = 0$ in (3.2) in this way results in the *layer problem*,

$$\begin{aligned} \frac{\mathrm{d}s}{\mathrm{d}z} &= 0, \\ \frac{\mathrm{d}n}{\mathrm{d}z} &= 0, \\ \frac{\mathrm{d}v}{\mathrm{d}z} &= f_1(s, n, v, t, 0), \\ \frac{\mathrm{d}t}{\mathrm{d}z} &= f_2(s, n, v, t, 0), \end{aligned} \tag{3.3}$$

in which the variables (s, n) are no longer dynamic and instead act as parameters in the resulting planar system

$$\begin{aligned} \frac{\mathrm{d}v}{\mathrm{d}z} &= f_1(s, n, v, t, 0), \\ \frac{\mathrm{d}t}{\mathrm{d}z} &= f_2(s, n, v, t, 0) \end{aligned} \tag{3.4}$$

for the "fast" variables (v, t), called the fast subsystem. This system has a set of equilibria, called the critical manifold, given by

$$\mathcal{S}_0 := \left\{(s, n, v, t) \in \mathbb{R}^4 : F(s, n, v, t, 0) = 0\right\}, \quad F(s, n, v, t, \varepsilon) := \begin{pmatrix} f_1(s, n, v, t, \varepsilon) \\ f_2(s, n, v, t, \varepsilon) \end{pmatrix}. \tag{3.5}$$

If we now set $\varepsilon = 0$ in (3.1), this results in the *reduced problem*:

$$\begin{aligned} \frac{\mathrm{d}s}{\mathrm{d}y} &= g_1(s,n,v,t,0), \\ \frac{\mathrm{d}n}{\mathrm{d}y} &= g_2(s,n,v,t,0), \\ 0 &= f_1(s,n,v,t,0), \\ 0 &= f_2(s,n,v,t,0), \end{aligned} \tag{3.6}$$

in which the flow is restricted to the critical manifold $\mathcal{S}_0$, and the dynamics on $\mathcal{S}_0$ are governed by the first two equations for the "slow" variables (s,n).

3.2. The layer problem. The flow for the layer problem (3.3) is restricted to planes of constant (s,n), in which any fixed point solutions must lie on the critical manifold. This manifold is a folded surface, formed by two branches of hyperbolic fixed points, one of which consists of saddle equilibria and the other of repelling equilibria separated by a fold curve of nonhyperbolic fixed points; see Figure 1. This is the content of the following.

Proposition 3.1. *The critical manifold $\mathcal{S}_0 = \mathcal{S}_0^{\mathrm{sub}} \cup \mathcal{F} \cup \mathcal{S}_0^{\mathrm{super}}$ is folded with a subsonic branch of hyperbolic saddle equilibria, $\mathcal{S}_0^{\mathrm{sub}}$, a sonic fold curve, $\mathcal{F}$, and a supersonic branch of hyperbolic repelling equilibria, $\mathcal{S}_0^{\mathrm{super}}$.*

Proof. We compute the linearization of (3.3) evaluated along the critical manifold. The critical manifold is found by simultaneously solving $f_1(s,n,v,t,0) = f_2(s,n,v,t,0) = 0$, and we note that by definition of φ in (2.22), we have that $\varphi(s,n,v,t,0) = f_2(s,n,v,t,0)$, so that $f_2(s,n,v,t,0) = 0$ precisely when φ vanishes. We therefore solve the first term of $f_1(s,n,v,t,0) = 0$ for $n = n(s,v,t)$ by setting

$$n = n(s,v,t(v,s)) := \frac{(\gamma-1)\sqrt{t(v,s)}}{s^2}\left(v + \frac{1}{\gamma v}\right), \tag{3.7}$$

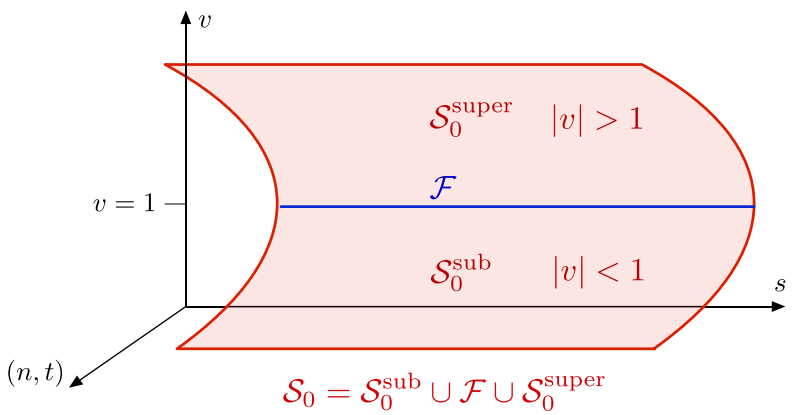

Figure 1. *Shown is the folded critical manifold $\mathcal{S}_0$, composed of a subsonic saddle branch $\mathcal{S}_0^{\mathrm{sub}}$ in the region $v < 1$ and a supersonic repelling branch $\mathcal{S}_0^{\mathrm{super}}$ in the region $v > 1$, separated by the sonic fold curve $\mathcal{F}$.*

where we obtain

$$t = t(v,s) := \frac{2(\alpha+s)}{s\left(v^2(\gamma-1)+2\right)}, \tag{3.8}$$

by substituting (3.7) into $f_2(s,n,v,t,0)=0$ and solving for $t=t(v,s)$. Using these expressions, and denoting by $J|_{\mathcal{S}_0}$ the Jacobian of the fast subsystem (3.4) evaluated along the critical manifold $\mathcal{S}_0$, we find that

$$J|_{\mathcal{S}_0} = \begin{pmatrix} \frac{3}{4\bar{\eta}(t)s^2}\left(1-\frac{1}{\gamma v^2}\right) - \frac{\theta(\gamma-1)}{2\gamma s^2\bar{\zeta}(t)} & \frac{v^2(\gamma-1)+2}{2s(\alpha+s)}\left(\frac{3}{8\bar{\eta}(t)}\left(v+\frac{1}{\gamma v}\right) - \frac{\theta v(\gamma+1)}{4\gamma\bar{\zeta}(t)}\right) \\ \\ \frac{\theta}{\bar{\zeta}(t)}\frac{2(\gamma-1)(\alpha+s)}{\gamma v s^3(v^2(\gamma-1)+2)} & \frac{\theta}{\bar{\zeta}(t)}\frac{\gamma+1}{2\gamma s^2} \end{pmatrix}, \tag{3.9}$$

from which we compute

$$\det J|_{\mathcal{S}_0} = \frac{3\theta}{4\bar{\zeta}(t)\bar{\eta}(t)\gamma s^4 v^2}(v^2-1), \tag{3.10}$$

$$\mathrm{Tr} J|_{\mathcal{S}_0} = \frac{1}{\gamma s^2}\left(\frac{3}{4\bar{\eta}(t)}\left(\gamma-\frac{1}{v^2}\right)+\frac{\theta}{\bar{\zeta}(t)}\right). \tag{3.11}$$

Noting that $\theta>0$ and $\gamma>1$, in the region $s,t,v>0$ we can therefore determine the stability type of the fixed points on the critical manifold as summarized in Table 1. ∎

We now examine the dependence of fixed points of (3.3) on the values of (s,n). Since any such point must lie on the critical manifold, on which $F(s,n,v,t,0)=0$, we can solve $f_1(s,n,v,t,0)=0$ for $t=t(s,n,v)$ to obtain

$$t = t(s,n,v) := \frac{n^2 s^4 v^2 \gamma^2}{(\gamma-1)^2(\gamma v^2+1)^2}. \tag{3.12}$$

Substituting this expression into $f_2(s,n,v,t,0)=0$, we recover a quadratic in γv^2,

$$(\gamma-1)\left((\alpha+s)(\gamma-1)-\frac{n^2s^5}{2}\right)\left(\gamma v^2\right)^2 + \left(2(\alpha+s)(\gamma-1)^2 - n^2s^5\gamma\right)\gamma v^2 + (\alpha+s)(\gamma-1)^2 = 0, \tag{3.13}$$

which can be solved explicitly for v as

$$v = v_{\pm}(s,n) := \left(\frac{n^2s^5\gamma - 2(\alpha+s)(\gamma-1)^2 \pm ns^2\sqrt{s\left(n^2s^5\gamma^2 - 2(\alpha+s)(\gamma+1)(\gamma-1)^2\right)}}{\gamma(\gamma-1)\left(2(\alpha+s)(\gamma-1)-n^2s^5\right)}\right)^{1/2}. \tag{3.14}$$

Table 1
Structure of the critical manifold $\mathcal{S}_0$.

$v<1$ (subsonic)	$\det J\|_{\mathcal{S}_0} < 0$	saddle-type
$v=1$	$\det J\|_{\mathcal{S}_0} = 0$	nonhyperbolic
$v>1$ (supersonic)	$\mathrm{Tr} J\|_{\mathcal{S}_0} > 0, \det J\|_{\mathcal{S}_0} > 0$	repelling

Substituting (3.14) into (3.12), and setting $t_\pm(s,n) := t(s,n,v_\pm(s,n))$, yields the location of each root as a function of (s,n), as desired.

In the following analysis, in order to construct a transonic solution which returns to subsonic speeds in the far field, we will require that there exist two distinct, real valued solutions to (3.13), with one subsonic solution and one supersonic (see section 3.4). This requirement requires a restriction on the possible values of (s,n) in the layer problem (3.3), as shown in the following lemma.

Lemma 3.2. *In order for there to exist two fixed points to the layer problem (3.3) in the region $v>0$ at a value of $s>0$, the variable n must satisfy*

$$\frac{\gamma^2-1}{\gamma^2} < \frac{n^2 s^5}{2(\alpha+s)(\gamma-1)} < 1. \tag{3.15}$$

Furthermore, under these conditions, we have that $v_-<1$ and $v_+>1$, so that one of the fixed points lies on the subsonic branch $\mathcal{S}_0^{\text{sub}}$ and the other on the supersonic branch $\mathcal{S}_0^{\text{super}}$.

Proof. In order for both of the roots of (3.13) to be real valued, the discriminant of the quadratic equation (3.13) must be positive, from which we obtain

$$\frac{n^2 s^5}{2(\alpha+s)(\gamma-1)} > \frac{\gamma^2-1}{\gamma^2}. \tag{3.16}$$

This inequality then implies

$$\frac{n^2 s^5}{2(\alpha+s)(\gamma-1)} > \frac{\gamma-1}{\gamma}, \tag{3.17}$$

so in order to obtain two real, positive roots $v_\pm$, the denominator in the expression (3.14) must be positive, so that

$$\frac{n^2 s^5}{2(\alpha+s)(\gamma-1)} < 1, \tag{3.18}$$

from which we obtain (3.15). The inequality (3.15) can be rearranged as

$$n_{\min}(s)^2 := 2\left(\frac{\alpha+s}{s^5}\right)\frac{(\gamma+1)(\gamma-1)^2}{\gamma^2} < n^2 < \frac{2(\gamma-1)(\alpha+s)}{s^5} =: n_{\max}(s)^2.$$

From the expression (3.14), we find that the value of $v_+(s,n)$ is increasing in n and is therefore minimized when $n^2 = n_{\min}(s)^2$. Thus,

$$\begin{aligned} &v_+(s,n) \\ &> \left(\frac{n^2 s^5\gamma - 2\,(\alpha+s)\,(\gamma-1)^2 \pm n s^2\sqrt{s\,(n^2 s^5\gamma^2 - 2(\alpha+s)(\gamma+1)(\gamma-1)^2)}}{\gamma(\gamma-1)\,(2(\alpha+s)(\gamma-1)-n^2 s^5)}\right)^{1/2}\Bigg|_{n^2=n_{\min}^2} \\ &= 1. \end{aligned}$$

Likewise, after some rearrangement of the expression (3.14) for $v_-(s,n)$, we find that

(3.19)
$$v_-(s,n) = \left(\frac{2\,(\alpha+s)\,(\gamma-1)^2}{\gamma\left(n^2 s^5 \gamma - 2\,(\alpha+s)\,(\gamma-1)^2 + n s^2 \sqrt{s\,(n^2 s^5 \gamma^2 - 2(\alpha+s)(\gamma+1)(\gamma-1)^2)}\right)} \right)^{1/2}$$

from which we see that $v_-(s,n)$ is decreasing in n and is therefore maximized when $n^2 = n_{\min}(s)^2$, from which we obtain

$$v_-(s,n) < 1$$

by a similar computation. ∎

3.3. The reduced problem. We recall from the proof of Proposition 3.1 that along the critical manifold $\mathcal{S}_0$, we can express

$$n = n\,(s, v, t(v,s)) := \frac{(\gamma-1)\sqrt{t(v,s)}}{s^2}\left(v + \frac{1}{\gamma v}\right), \tag{3.20}$$

where

$$t(v,s) := \frac{2(\alpha+s)}{s\,(v^2(\gamma-1)+2)}. \tag{3.21}$$

Substituting these expressions into (3.6) yields equations for the reduced dynamics on the critical manifold in terms of (s,v) as

$$\begin{aligned} \frac{\mathrm{d}s}{\mathrm{d}y} &= 1, \\ \frac{\mathrm{d}v}{\mathrm{d}y} &= \frac{1}{s(1-v^2)}\left(\frac{\alpha}{4}\frac{5-3\gamma}{\gamma-1} - s\right)\left(\frac{v(v^2(\gamma-1)+2)}{\alpha+s}\right). \end{aligned} \tag{3.22}$$

The corresponding dynamics for the value $\gamma = 1.4$ are shown in Figure 2.

Note that the system is singular at $s = 0$ and $v = \pm 1$. To remedy this, we desingularize the reduced dynamics by rescaling $\mathrm{d}y = s(1-v^2)\mathrm{d}\bar{y}$, resulting in the system

$$\begin{aligned} \frac{\mathrm{d}s}{\mathrm{d}\bar{y}} &= s(1-v^2), \\ \frac{\mathrm{d}v}{\mathrm{d}\bar{y}} &= \left(\frac{\alpha}{4}\frac{5-3\gamma}{\gamma-1} - s\right)\left(\frac{v(v^2(\gamma-1)+2)}{\alpha+s}\right). \end{aligned} \tag{3.23}$$

The phase portraits of the systems (3.22) and (3.23) are identical in the region $s > 0$, up to a change of orientation in the supersonic region $v^2 > 1$. Computing $\frac{\mathrm{d}v}{\mathrm{d}s}$ from (3.23) (or equivalently (3.22)) results in a separable equation which can be integrated to reveal that (3.23) is conservative with level sets

$$E(s,v) := \frac{\ln(v)}{2} - \frac{(\gamma+1)\ln(v^2(\gamma-1)+2)}{4(\gamma-1)} - \frac{\ln(s)}{\alpha} + \frac{(\alpha+1)\ln(\alpha+s)}{\alpha}. \tag{3.24}$$

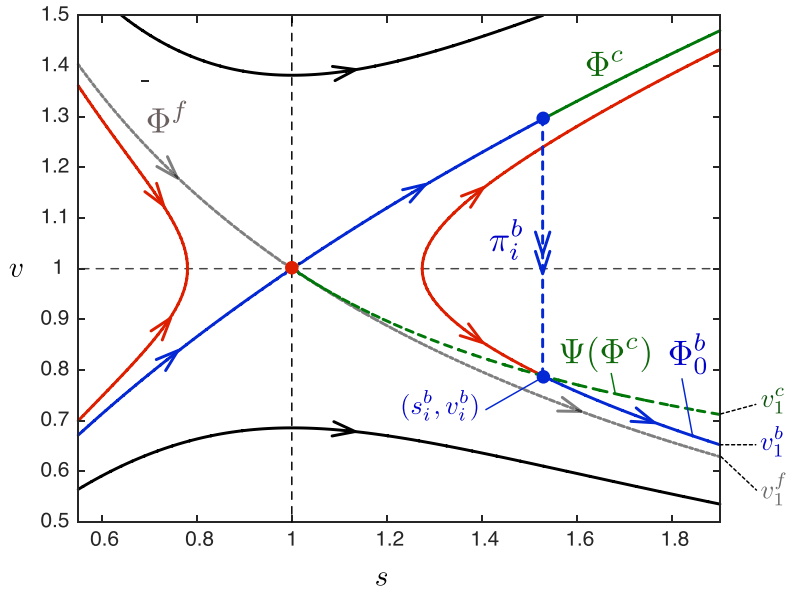

Figure 2. *Shown is the reduced flow on the critical manifold $\mathcal{S}_0$ for $\gamma = 1.4$, $s_0 = 0.55, s_1 = 1.9$. The true and faux canards Φ^f, Φ^c correspond to the energy level set $E(s,v) = E_0$ and intersect at the sonic point $(s,v) = (1,1)$. Also shown are the level sets corresponding to $E(s,v) = E_0 - 0.05$ (black) and $E(s,v) = E_0 + 0.01$ (red). Note that the latter level set is crossed transversely by the projected canard $\Psi(\Phi^c)$ in the region $s > 1$. The singular transonic solution $\Phi_0 = \Phi^c \cup \pi_i^b \cup \Phi_0^b$ is formed by (a portion of) the canard orbit Φ^c, followed by the fast jump π_i^b, and then the slow trajectory Φ_0^b on the subsonic branch $\mathcal{S}_0^{\text{sub}}$ satisfying $v = v_1^b$ at $s = s_1$.*

Additionally, the desingularized system (3.23) admits a fixed point, called a folded singularity [37], which is located at

$$(s^*, v^*) = \left(\frac{\alpha(5 - 3\gamma)}{4(\gamma - 1)}, 1 \right). \tag{3.25}$$

We will see in the following analysis that this folded singularity allows for the smooth transition from subsonic to supersonic speeds for small $\varepsilon > 0$, and we therefore refer to this as the *sonic point*. We now choose the (previously undetermined) scaling

$$\alpha := \frac{4(\gamma - 1)}{5 - 3\gamma} > 0$$

for convenience, so that the location of the sonic point is fixed at

$$(s^*, v^*) = (1, 1) \tag{3.26}$$

for all values of $\gamma \in (1, 5/3)$. We have the following.

Proposition 3.3. *The folded singularity is of saddle type for all values of $\gamma \in (1, 5/3)$.*

Proof. We calculate the linearization of the desingularized system (3.23) at the folded singularity (3.26) as

$$J_{\text{fs}} = \left(\begin{array}{cc} 1-v^2 & -2sv \\ -\frac{v\left(v^2(\gamma-1)+2\right)(\alpha+1)}{(\alpha+s)^2} & \frac{(1-s)\left(3v^2(\gamma-1)+2\right)}{\alpha+s} \end{array} \right) \Bigg|_{(s,v)=(s^*,v^*)}$$

$$= \begin{pmatrix} 0 & -2 \\ -(5-3\gamma) & 0 \end{pmatrix}. \tag{3.27}$$

We have that

$$\det J_{\text{fs}} = -2(5-3\gamma) < 0 \quad \text{for } \gamma \in (1, 5/3) \tag{3.28}$$

so that the folded singularity (3.26) is a folded saddle [37]. ∎

Associated with this folded saddle singularity are a pair of canard orbits, one which traverses the sonic point from the subsonic branch to the supersonic branch as s increases, and one which crosses the sonic point moving from supersonic to subsonic [37]. The former, which we denote by Φ^c, is referred to as the "true" canard, while the latter, which we denote by Φ^f, is sometimes called a "faux" canard. The distinguished true canard orbit Φ^c provides a means of accelerating from subsonic to supersonic speeds along the critical manifold via the sonic point.

3.4. Construction of singular orbits. By combining orbits from the layer and reduced problems, discussed in sections 3.2–3.3, we are able to construct singular orbits, which will serve as candidates for transonic stellar wind solutions of the full problem (3.1) for $0 < \varepsilon \ll 1$. We recall from section 2.2 that a transonic stellar wind solution must be subsonic at the stellar surface, which we denote by $s = s_0$ in the rescaled radial coordinate, accelerating to supersonic speeds in a bounded region in space, before returning to subsonic speeds in the far field. Stated in the rescaled variables (s, v), this means that a transonic stellar wind solution $(v(s), n(s), t(s))$, on the interval $s \in (s_0, \infty)$, must satisfy the following:

(i) The velocity $v(s)$ is subsonic ($v < 1$) at the inner boundary $s = s_0$ and asymptotically subsonic as $s \to \infty$.

(ii) $v(s)$ is supersonic ($v > 1$) for $s \in \tilde{I}$, where $\tilde{I} \subset (s_0, \infty)$ is a bounded interval.

To build such a solution, we note that in the limiting singular systems, for a solution which is subsonic at the surface $s = s_0$, the only means of accelerating to supersonic speeds is via the canard orbit Φ^c which crosses the sonic point on the critical manifold $\mathcal{S}_0$. If $s_0 > 1$, then no such orbit exists; hence we assume $s_0 < 1$. In order for a supersonic solution to return to subsonic speeds as $s \to \infty$, we recall from Proposition 3.1 that the upper supersonic branch $\mathcal{S}_0^{\text{super}}$ is normally repelling, while the lower subsonic branch is of saddle type. Therefore it will be possible to transition from $\mathcal{S}_0^{\text{super}}$ to $\mathcal{S}_0^{\text{sub}}$ provided there exists a heteroclinic orbit of the layer problem (3.3) which connects the repelling supersonic fixed point to the corresponding saddle-type subsonic fixed point within the same (s, n)-slice. This fast heteroclinic orbit will manifest as a viscous shock in the perturbed solution. Once the solution returns to $\mathcal{S}_0^{\text{sub}}$ in the region $s > 1$, it will be possible to follow one of the singular reduced orbits which satisfies $0 < v < 1$ as $s \to \infty$.

We therefore construct candidate singular orbits in three pieces $\Phi_0 = \Phi_0^c \cup \pi_i^b \cup \Phi_0^b$ (see Figures 2 and 3), where Φ_0^b is an orbit of the reduced system (3.6) on $\mathcal{S}_0^{\text{sub}}$ with appropriate

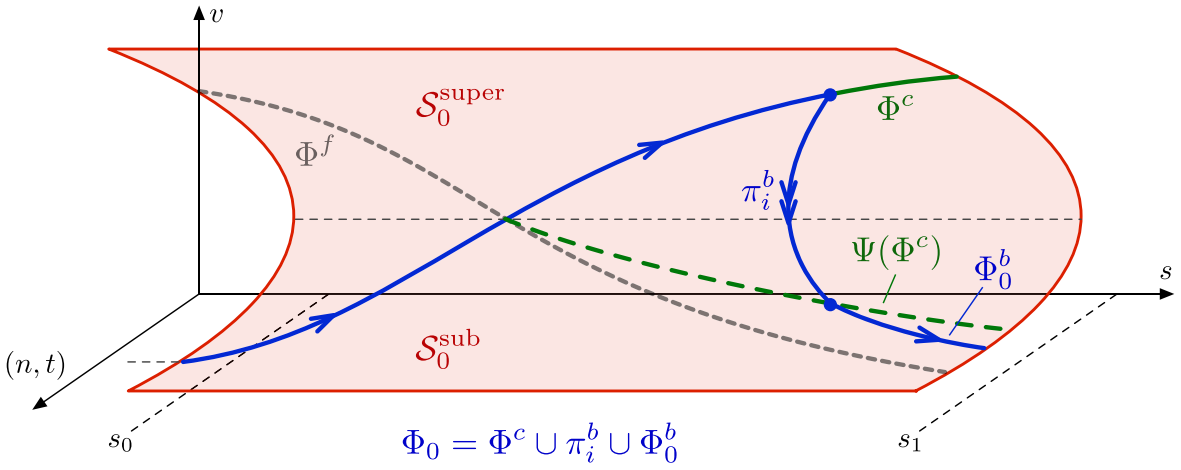

Figure 3. *Shown is a schematic for the construction of a singular transonic solution Φ_0 on a bounded interval $s \in (s_0, s_1)$. The solution consists of three trajectories $\Phi_0 = \Phi^c \cup \pi_i^b \cup \Phi_0^b$, where Φ^c is the canard on the critical manifold $\mathcal{S}_0$ which accelerates from sub- to supersonic speeds via the sonic point, π_i^b is the fast heteroclinic orbit from Proposition 3.4 which defines the projection $\Psi\colon \mathcal{S}_0^{\text{super}} \to \mathcal{S}_0^{\text{sub}}$, and Φ_0^b is a slow trajectory on the subsonic branch $\mathcal{S}_0^{\text{sub}}$ with the appropriate boundary condition $v = v_1^b$ at $s = s_1$.*

far-field boundary conditions as $s \to \infty$, and π_i^b is a fast heteroclinic orbit which connects Φ_0^c to Φ_0^b, provided such an orbit exists. We will then perturb from Φ_0 for $0 < \varepsilon \ll 1$ to obtain a solution of the full problem (3.1).

To construct the orbit π_i^b, we return to the desingularized system (3.23), which we recall is conservative with conserved quantity $E(s, v)$ defined in (3.24). The canard solutions Φ^c and Φ^f lie on the level set

$$E(1,1) = \frac{(\gamma+1)}{4(\gamma-1)} \ln\left(\frac{1}{5-3\gamma}\right) =: E_0. \tag{3.29}$$

This level set divides the phase portrait of (3.23) into four regions: in the regions to the left and right of the two canard curves Φ^c and Φ^f, we have $E > E_0$, while the regions above and below both Φ^c and Φ^f satisfy $E < E_0$.

In order to find an orbit which jumps from the canard Φ^c on $\mathcal{S}_0^{\text{super}}$ for $s > 1$ to the subsonic branch $\mathcal{S}_0^{\text{sub}}$, there must exist a heteroclinic orbit of the layer problem (3.3) between the unstable fixed point on $\mathcal{S}_0^{\text{super}}$ and the corresponding saddle point on $\mathcal{S}_0^{\text{sub}}$. We recall from section 3.2 that these fixed points of (3.3) are denoted by $(v_\pm(s,n), t_\pm(s,n))$ where $v = v_\pm$ satisfy (3.14), with corresponding temperatures given by (3.12) as

$$t_\pm(s,n) = \frac{n^2 s^4 v_\pm^2 \gamma^2}{(\gamma-1)^2(\gamma v_\pm^2 + 1)^2}. \tag{3.30}$$

We also recall from Lemma 3.2 that $v_+ > 1$ and $v_- < 1$, so that (v_+, t_+) corresponds to the repelling (supersonic) fixed point and (v_-, t_-) corresponds to the (subsonic) saddle point.

We have the following proposition, which is proved in Appendix A.

Proposition 3.4. *For any $\gamma \in (1, 5/3)$, and any $s > 1$ and $n > 0$ satisfying the bounds in Lemma 3.2, there exists a heteroclinic orbit in the layer problem (3.3) connecting $(v_+, t_+) \in \mathcal{S}_0^{\text{super}}$ to $(v_-, t_-) \in \mathcal{S}_0^{\text{sub}}$.*

The idea of the proof is to establish a trapping region of (3.3) using its nullclines. We show that the flow of (3.3) in forward time is directed out of the region, thus creating a trapping region under the reverse flow (see Figure 4); the result then follows from the Poincaré–Bendixson theorem.

We can now define a projection $\Psi\colon \mathcal{S}_0^{\text{super}} \to \mathcal{S}_0^{\text{sub}}$ to be the map that projects a point on the supersonic repelling branch to the subsonic saddle branch via a heteroclinic orbit, the existence of which is guaranteed by Proposition 3.4. Thus, we can define the projection Ψ via

$$\Psi(s, n, v_+(s,n), t_+(s,n)) = (s, n, v_-(s,n), t_-(s,n)). \tag{3.31}$$

Lemma 3.5. *The projection $\Psi(\Phi^c)$ for $s > 1$ lies above the faux canard Φ^f on $\mathcal{S}_0^{\text{sub}}$, so that $\Psi(\Phi^c)$ is confined to the region $E > E_0$. Furthermore, the trajectory $\Psi(\Phi^c)$ crosses level sets $E(s, n) =$ constant transversely.*

Proof. Any solution to the reduced problem satisfies $E(s, v) =$ constant. Using Vieta's formulas and (3.13), the quantity v_- can be represented in term of v_+ as

$$v_-^2 = \frac{2 + (\gamma - 1)v_+^2}{2\gamma v_+^2 - (\gamma - 1)}. \tag{3.32}$$

We can replace $v \to v_-$ as defined in (3.32) to compute the value of E along the projection $\Psi(\Phi^c)$ as a function of (s, v_+). We compute that

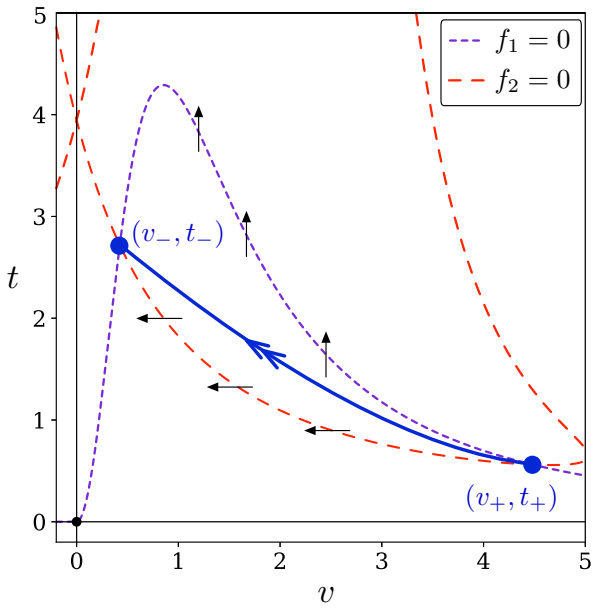

Figure 4. *Shown are the nullclines of the layer problem for $\gamma = 1.4$, $n = 1.15$, $s = 1.1$, and $\theta = 0.04$. Note that the saddle equilibrium is located where $v < 1$, and the unstable fixed point is in the $v > 1$ regime.*

$$\frac{\mathrm{d}E(s,v_-)}{\mathrm{d}y} = \frac{2\gamma(s-1)(v_+^2-1)}{s(\alpha+s)\left(2\gamma v_+^2-(\gamma-1)\right)} > 0$$

in the region $s > 1$ since $v_+^2 > 1$. Thus the value of E along the projection $\Psi(\Phi^c)$ is strictly increasing for $s > 1$, so that $\Psi(\Phi^c)$ cross level sets transversely on $\mathcal{S}_0^{\mathrm{sub}}$. This also immediately implies $E|_{\Psi(\Phi^c)} > E_0$, so that $\Psi(\Phi^c)$ lies above the faux canard trajectory Φ_0^f. ∎

We now complete the construction of solutions to (3.1) on bounded intervals for $0 < \varepsilon \ll 1$. We recall that the sonic point is located at $(s,v) = (1,1)$. We fix the bounded domain $s \in [s_0, s_1]$ with $s_0 < 1 < s_1$. We define v_0^c to be the v coordinate of the canard solution Φ^c at $s = s_0$. Note that $v_0^c < 1$. Likewise, we define v_1^c and v_1^f to be the v coordinates of the projected canard solution $\Psi(\Phi^c)$ and the faux canard solution Φ^f, respectively, at $s = s_1$. Note that both $v_1^c < 1$ and $v_1^f < 1$.

For every $v_1^b \in (v_1^f, v_1^c)$ there exists a solution to the layer problem Φ_0^b which meets $s = s_1$ at $v = v_1^b$. By Lemma 3.5 this solution intersects $\Psi(\Phi^c)$ transversely at some $v = v_i^b > 1$ and $s = s_i^b$ satisfying $1 < s_i^b < s_1$; the transversality of the intersection follows from the fact that solutions in the region bounded above by Φ^c and below by Φ^f lie on level sets of $E > E_0$, and E is increasing along the projected canard $\Psi(\Phi^c)$. Let n_i^b and t_i^b be the n and t coordinates, respectively, of the intersection of Φ^b and $\Psi(\Phi^c)$. Using the projection formula (3.32), and the fact that the v coordinate along $\Psi(\Phi^c)$ decreases in s, we have that $v_i^b > \frac{\gamma-1}{2\gamma}$.

A short computation then shows that n_i^b satisfies the bounds in Lemma 3.2, and thus by Proposition 3.4 there exists a fast heteroclinic orbit, which we denote by π_i^b, which connects the repelling branch $\mathcal{S}_0^{\mathrm{super}}$ to the saddle branch at $(s_i^b, n_i^b, v_i^b, t_i^b)$ via the projection Ψ. Furthermore, by construction, we have that $\Psi^{-1}(s_i^b, n_i^b, v_i^b, t_i^b) \in \mathcal{S}_0^{\mathrm{super}}$ lies on the canard orbit Φ^c. Therefore, tracing backward along Φ^c yields a singular transonic canard solution $\Phi_0 = \Phi^c \cup \pi_i^b \cup \Phi_0^b$—see Figure 2.

Additionally, we have that for each $v_1^b \in (0, v_1^f)$, there exists a trajectory Φ^b of the reduced flow that remains subsonic for all $s \in [s_0, s_1]$; the trajectory at $s = s_0$ approaches $v = v_0^b$, where $v_0^b \in (0, v_0^c)$, and approaches $v = v_1^b$ at $s = s_1$. We have the following proposition regarding the existence of stellar wind solutions on bounded domains.

Proposition 3.6. *Fix $s_0 < 1 < s_1$ and $\gamma \in (1, 5/3)$, with v_0^c, v_0^f, v_1^c, and v_1^f as defined above, and consider the system (3.2).*

(i) *Let $v_1^b \in (0, v_1^f)$ and let $\Phi_0 = \Phi_0^b$ be the singular subsonic trajectory which approaches $v = v_1^b$ at $s = s_1$. For each sufficiently small $\varepsilon > 0$, Φ_0 perturbs to a solution Φ_ε of (3.2) which is $\mathcal{O}(\varepsilon)$-close to Φ_0.*

(ii) *Let $v_1^b \in (v_1^f, v_1^c)$ and let $\Phi_0 = \Phi^c \cup \pi_i^b \cup \Phi_0^b$ be the singular trajectory that follows Φ^c from $s = s_0$ to $s = s_i^b$, traverses the fast layer orbit π_i^b at $s = s_i^b$, and then follows the trajectory Φ^b from $s = s_i^b$ to $s = s_1$. Then for sufficiently small $\varepsilon > 0$, Φ_0 perturbs to a solution Φ_ε of (3.2) which is $\mathcal{O}(\varepsilon^{1/2})$-close to Φ_0.*

4. Existence of transonic canard solutions for $0 < \varepsilon \ll 1$. In order to prove Proposition 3.6, we must first analyze the dynamics near the sonic point to determine how the canard trajectory Φ^c perturbs for small $\varepsilon > 0$. Using a center manifold reduction procedure as in [39],

we show that near the sonic point, the system (3.2) admits a three-dimensional center manifold on which the results of [37] concerning the persistence of canard trajectories apply.

4.1. Center manifold reduction near the sonic point. For $\varepsilon = 0$, the sonic point, corresponding to the folded saddle singularity of the reduced flow (3.23), is located at $(s, v) = (s^*, v^*) = (1, 1)$ on the critical manifold. We determine the corresponding (n, t)-coordinates via (3.20)–(3.21) as

$$\begin{aligned} t^* &= t(1,1) = \frac{2}{5-3\gamma}, \\ n^* &= n(1,1,t^*) = \frac{\gamma^2-1}{\gamma}\sqrt{\frac{2}{5-3\gamma}}. \end{aligned} \tag{4.1}$$

The linearization of (3.2) at $(s, n, v, t) = (1, n^*, 1, t^*)$ for $\varepsilon = 0$ admits a triple zero eigenvalue with a corresponding three-dimensional eigenspace spanned by the two slow directions $(1, 0, 0, 0)^T, (0, 1, 0, 0)^T$, and the eigenvector

$$\mathbf{v}_1 := \begin{pmatrix} 0 \\ 0 \\ -\frac{(\gamma+1)(5-3\gamma)}{4(\gamma-1)} \\ 1 \end{pmatrix} \tag{4.2}$$

as well as a positive eigenvalue

$$\lambda_+ := \frac{1}{\gamma}\left(\frac{3\,(\gamma-1)}{4\bar{\eta}(t^*)} + \frac{\theta}{\bar{\zeta}(t^*)}\right) \tag{4.3}$$

with corresponding eigenvector

$$\mathbf{v}_2 := \begin{pmatrix} 0 \\ 0 \\ -\frac{(5-3\gamma)(2\theta-3)}{8\theta} \\ 1 \end{pmatrix}. \tag{4.4}$$

Hence by the center manifold theorem, near the sonic point there exists a locally invariant normally repelling three-dimensional center manifold $\mathcal{W}^{\mathrm{c}}_{\mathrm{sp}}$ tangent to the subspace spanned by the vectors $(1, 0, 0, 0)^T, (0, 1, 0, 0)^T$, and $\mathbf{v}_1$. This manifold persists as a locally invariant repelling center manifold for $0 < \varepsilon \ll 1$ in a neighborhood of the sonic point, foliated by strong unstable fibers which are tangent to $\mathbf{v}_2$ at the sonic point. Within this center manifold, we have the following. The proof and additional details are given in Appendix B.

Proposition 4.1 ([37, Theorem 4.1]). *On the center manifold $\mathcal{W}^{\mathrm{c}}_{\mathrm{sp}}$, for all sufficiently small $\varepsilon > 0$, the repelling and saddle branches, $\mathcal{S}^{\mathrm{super}}_{\varepsilon}$ and $\mathcal{S}^{\mathrm{sub}}_{\varepsilon}$, break transversely and intersect along the maximal canard solution $\Phi^{\mathrm{c}}_{\varepsilon}$, which is $\mathcal{O}(\varepsilon^{1/2})$-close to the corresponding singular canard solution Φ^{c}.*

4.2. Existence of canard solutions on bounded intervals. In this section, we complete the construction of transonic canards on bounded intervals.

Proof of Proposition 3.6. For (i), let σ_1^b denote the intersection point of Φ_0 with the subspace $s = s_1$. We choose any one-dimensional boundary manifold Σ_1 which for $\varepsilon = 0$ transversely intersects the unstable manifold $\mathcal{W}^{\mathrm{u}}(\mathcal{S}_0^{\mathrm{sub}})$ of $\mathcal{S}_0^{\mathrm{sub}}$ at σ_1^b within the subspace $s = s_1$.

Since $\Phi_0 = \Phi_0^b$ is subsonic for $s \in (s_0, s_1)$, the entire orbit Φ_0 lies on $\mathcal{S}_0^{\mathrm{sub}}$ and is bounded away from the fold curve. Further, $\mathcal{S}_0^{\mathrm{sub}}$ is normally hyperbolic away from the fold curve, and therefore Fenichel theory implies that $\mathcal{S}_0^{\mathrm{sub}}$ perturbs for sufficiently small $\varepsilon > 0$ to a normally hyperbolic slow manifold $\mathcal{S}_\varepsilon^{\mathrm{sub}}$, and the flow on $\mathcal{S}_\varepsilon^{\mathrm{sub}}$ is an $\mathcal{O}(\varepsilon)$ perturbation of the reduced flow (3.6) on $\mathcal{S}_0^{\mathrm{sub}}$; in particular the orbit Φ_0^b perturbs to an orbit Φ_ε^b on $\mathcal{S}_\varepsilon^{\mathrm{sub}}$. However, this orbit may not satisfy the desired boundary conditions, so we instead find a perturbed solution which meets the boundary manifold Σ_1 at $s = s_1$.

To this end, the three-dimensional unstable and stable manifolds $\mathcal{W}^{\mathrm{u}}(\mathcal{S}_0^{\mathrm{sub}})$ and $\mathcal{W}^{\mathrm{s}}(\mathcal{S}_0^{\mathrm{sub}})$ of $\mathcal{S}_0^{\mathrm{sub}}$ perturb to three-dimensional locally invariant manifolds $\mathcal{W}^{\mathrm{u}}(\mathcal{S}_\varepsilon^{\mathrm{sub}})$ and $\mathcal{W}^{\mathrm{s}}(\mathcal{S}_\varepsilon^{\mathrm{sub}})$, respectively, foliated by the perturbed strong unstable/stable fibers of orbits on the slow manifold $\mathcal{S}_\varepsilon^{\mathrm{sub}}$. Thus the transversality of the intersection of Σ_1 and the unstable manifold $\mathcal{W}^{\mathrm{u}}(\mathcal{S}_\varepsilon^{\mathrm{sub}})$ in the subspace $s = s_1$ persists, with the intersection occurring in the strong unstable fiber of a solution $\mathcal{O}(\varepsilon)$-close to Φ_0^b. Tracing the intersection of Σ_1 and $\mathcal{W}^{\mathrm{u}}(\mathcal{S}_\varepsilon^{\mathrm{sub}})$ backward under the flow of (3.2) thus yields a one-dimensional trajectory Φ_ε, which is $\mathcal{O}(\varepsilon)$-close to Φ_0 and lies in the one-dimensional boundary manifold Σ_1 at $s = s_1$.

For (ii), we first note that Lemma 3.5 guarantees that the curves $\Psi(\Phi^c)$ and Φ_0^b intersect transversely on $\mathcal{S}_0^{\mathrm{sub}}$ for $\varepsilon = 0$. It immediately follows that the three-dimensional unstable fiber $\mathcal{W}^{\mathrm{u}}(\Phi^c)$ of the singular canard trajectory Φ_0^c transversely intersects the two-dimensional stable fiber $\mathcal{W}^{\mathrm{s}}(\Phi_0^b)$ of Φ_0^b along the fast jump π_i^b for $\varepsilon = 0$. To construct a solution for $\varepsilon > 0$ with the desired boundary conditions, we define two boundary manifolds, Σ_0 at $s = s_0$ and Σ_1 at $s = s_1$, and evolve these forward and backward, respectively, under the flow of (3.2) for $\varepsilon > 0$ and show that the evolved manifolds are close to $\mathcal{W}^{\mathrm{u}}(\Phi^c)$ and $\mathcal{W}^{\mathrm{s}}(\Phi_0^b)$, respectively, near the fast jump π_0^b and hence also intersect transversely along the desired solution for $\varepsilon > 0$.

We define the one-dimensional boundary manifold Σ_1 at $s = s_1$ the same as above in the proof of (i). Since Σ_1 intersects $\mathcal{W}^{\mathrm{u}}(\mathcal{S}_0^{\mathrm{sub}})$ transversely for $\varepsilon = 0$, this intersection persists for $\varepsilon > 0$ by Fenichel theory. Following Σ_1 backward under the flow of (3.2) traces out a two-dimensional manifold $\bar{\Sigma}_1$, which, upon entering a neighborhood of $s = s_i^b$, aligns exponentially close to the unstable fiber of a slow trajectory on $\mathcal{S}_\varepsilon^{\mathrm{sub}}$, which is $\mathcal{O}(\varepsilon)$-close to Φ_0^b. Therefore, $\bar{\Sigma}_1$ is $\mathcal{O}(\varepsilon)$-close to $\mathcal{W}^{\mathrm{u}}(\Phi_0^b)$ near $s = s_i^b$.

Within the subspace $s = s_0$, we take any two-dimensional boundary manifold Σ_0 which transversely intersects $\mathcal{W}^{\mathrm{s}}(\mathcal{S}_\varepsilon^{\mathrm{sub}})$ at the point σ_ε^c, where σ_ε^c denotes the location of the perturbed canard orbit Φ_ε^c at $s = s_0$. Away from the fold, the repelling and saddle branches of the critical manifold, $\mathcal{S}_0^{\mathrm{super}}$ and $\mathcal{S}_0^{\mathrm{sub}}$, respectively, are normally hyperbolic and therefore for sufficiently small $\varepsilon > 0$ perturb to locally invariant manifolds $\mathcal{S}_\varepsilon^{\mathrm{super}}$ and $\mathcal{S}_\varepsilon^{\mathrm{sub}}$, as do their stable and unstable foliations. Evolving Σ_0 forward under the flow of (3.2) along Φ_ε^c therefore traces out a three-dimensional manifold $\bar{\Sigma}_0$, which by the exchange lemma [22] aligns exponentially close to $\mathcal{W}^{\mathrm{u}}(\mathcal{S}_\varepsilon^{\mathrm{sub}})$ upon entering the neighborhood of the sonic point.

To determine how $\bar{\Sigma}_0$ traverses the sonic point, we note that by Proposition 4.1, in a neighborhood of the sonic point, for sufficiently small $\varepsilon > 0$, $\mathcal{S}_\varepsilon^{\mathrm{super}}$ and $\mathcal{S}_\varepsilon^{\mathrm{sub}}$ intersect transversely

along the perturbed maximal canard Φ_ε^c, which is $\mathcal{O}(\varepsilon^{1/2})$-close to the singular canard Φ_0^c, and thus passes $\mathcal{O}(\varepsilon^{1/2})$-close to the sonic point. Thus, in this neighborhood, $\bar{\Sigma}_0$ aligns with the strong unstable foliation $\mathcal{W}^{\mathrm{uu}}(S_\varepsilon^{\mathrm{sub}})$ of $\mathcal{S}_\varepsilon^{\mathrm{sub}}$, where trajectories on $\mathcal{S}_\varepsilon^{\mathrm{sub}}$ shadow orbits on the center manifold $\mathcal{W}_{\mathrm{sp}}^{\mathrm{c}}$, and the foliation $\mathcal{W}^{\mathrm{uu}}(S_\varepsilon^{\mathrm{sub}})$ is with respect to the strong unstable $\mathbf{v}_2$-direction. Since $\mathcal{S}_\varepsilon^{\mathrm{sub}}$ and $\mathcal{S}_\varepsilon^{\mathrm{super}}$ intersect transversely along the maximal canard Φ_ε^c, and $\bar{\Sigma}_0$ is exponentially close to $\mathcal{S}_\varepsilon^{\mathrm{sub}}$, we have that $\bar{\Sigma}_0$ intersects $\mathcal{S}_\varepsilon^{\mathrm{super}}$ transversely in the neighborhood of the sonic point. After passing through the sonic point, by the exchange lemma $\bar{\Sigma}_0$ aligns exponentially close to the unstable fibers of the maximal canard Φ_ε^c upon entry into the neighborhood of the subspace $s = s_i^b$; hence $\bar{\Sigma}_0$ is $\mathcal{O}(\varepsilon)$-close to $\mathcal{W}^{\mathrm{u}}(\Phi_\varepsilon^c)$ near $s = s_i^b$.

Since the intersection of $\mathcal{W}^{\mathrm{u}}(\Phi_0^c)$ and $\mathcal{W}^{\mathrm{s}}(\Phi_0^b)$ along π_0^b is transverse for $\varepsilon = 0$, for sufficiently small $\varepsilon > 0$, the transversality of the intersection persists. Thus, $\bar{\Sigma}_0$ and $\bar{\Sigma}_1$ intersect along an orbit Φ_ε which is $\mathcal{O}(\varepsilon^{1/2})$-close to Φ_0, as desired. ∎

4.3. Boundary manifolds at infinity. While Proposition 3.6 concerns the construction of stellar wind solutions on bounded domains, the proof of Proposition 3.6 is valid for any suitable choice of one-dimensional boundary manifold Σ_1 in the subspace $s = s_1$, which transversely intersects $\mathcal{W}^{\mathrm{u}}(\mathcal{S}_0^{\mathrm{sub}})$. This guarantees the existence of a stellar wind solution which satisfies prescribed boundary conditions at some finite radius from the star. We now show that it is possible to choose this boundary manifold in such a way that the stellar wind asymptotically approaches the prescribed far field boundary conditions as $s \to \infty$. To achieve this, we construct invariant far-field boundary manifolds at $s = \infty$, and we show that when these manifolds are transported back to $s = s_1$ for some $s_1 \gg 1$, we obtain boundary manifolds in the subspace $s = s_1$ which satisfy the conditions required by Σ_1 in the proof of Proposition 3.6.

We first consider the system (3.2) near $s = \infty$. To do this, we define $\sigma = 1/s$, from which we obtain

$$
\begin{aligned}
\frac{\mathrm{d}\sigma}{\mathrm{d}y} &= -\sigma^2, \\
\frac{\mathrm{d}n}{\mathrm{d}y} &= -2(\gamma-1)v\sqrt{t}\sigma^3 - \frac{\alpha\sigma^4}{v\sqrt{t}} - 4(\gamma-1)v\sqrt{t}\sigma\bar{\eta}'(t)\tilde{\varphi}(\sigma,n,v,t,\epsilon), \\
\varepsilon\frac{\mathrm{d}v}{\mathrm{d}y} &= \frac{3}{4\bar{\eta}(t)}\left(v\sigma^2 + \frac{\sigma^2}{\gamma v} - \frac{1}{\gamma-1}\frac{n}{\sqrt{t}}\right) - 2\varepsilon v\sigma - \frac{v}{2t}\tilde{\varphi}(\sigma,n,v,t,\varepsilon), \\
\varepsilon\frac{\mathrm{d}t}{\mathrm{d}y} &= \frac{\theta}{\bar{\zeta}(t)}\left(vn\sqrt{t} - \frac{\gamma-1}{2}v^2t\sigma^2 - \alpha\sigma^3 + \frac{1}{\gamma}t\sigma^2 - \sigma^2 + 4\varepsilon(\gamma-1)\bar{\eta}(t)v^2t\sigma\right),
\end{aligned}
\tag{4.5}
$$

where the asymptotic behavior as $s \to \infty$ is now determined by the limit $\sigma \to 0$, and the quantity $\tilde{\varphi}(\sigma,n,v,t,\varepsilon) := \varphi(\sigma^{-1},n,v,t,\varepsilon)$ denotes the right-hand side of the t-equation

$$
\tilde{\varphi}(\sigma,n,v,t,\varepsilon) = \frac{\theta}{\bar{\zeta}(t)}\left(vn\sqrt{t} - \frac{\gamma-1}{2}v^2t\sigma^2 - \alpha\sigma^3 + \frac{1}{\gamma}t\sigma^2 - \sigma^2 + 4\varepsilon(\gamma-1)\bar{\eta}(t)v^2t\sigma\right). \tag{4.6}
$$

We switch to the fast timescale and obtain

$$
\begin{aligned}
\frac{\mathrm{d}\sigma}{\mathrm{d}z} &= -\varepsilon\sigma^2, \\
\frac{\mathrm{d}n}{\mathrm{d}z} &= \varepsilon\left(-2(\gamma-1)v\sqrt{t}\sigma^3 - \frac{\alpha\sigma^4}{v\sqrt{t}} - 4(\gamma-1)v\sqrt{t}\sigma\bar{\eta}'(t)\tilde{\varphi}(\sigma,n,v,t,\epsilon)\right),
\end{aligned}
\tag{4.7}
$$

$$\frac{\mathrm{d}v}{\mathrm{d}z} = \frac{3}{4\bar{\eta}(t)}\left(v\sigma^2 + \frac{\sigma^2}{\gamma v} - \frac{1}{\gamma-1}\frac{n}{\sqrt{t}}\right) - 2\varepsilon v\sigma - \frac{v}{2t}\tilde{\varphi}(\sigma,n,v,t,\varepsilon),$$
$$\frac{\mathrm{d}t}{\mathrm{d}z} = \frac{\theta}{\bar{\zeta}(t)}\left(vn\sqrt{t} - \frac{\gamma-1}{2}v^2t\sigma^2 - \alpha\sigma^3 + \frac{1}{\gamma}t\sigma^2 - \sigma^2 + 4\varepsilon(\gamma-1)\bar{\eta}(t)v^2t\sigma\right).$$

We now perform the blow-up rescaling $v = \sigma^2\bar{v}$ and $\mathrm{d}z = \sigma^2\mathrm{d}\bar{z}$ to obtain the system

$$\begin{aligned}
\frac{\mathrm{d}\sigma}{\mathrm{d}\bar{z}} &= -\varepsilon\sigma^4,\\
\frac{\mathrm{d}n}{\mathrm{d}\bar{z}} &= \varepsilon\sigma^2\left(-2(\gamma-1)\bar{v}\sqrt{t}t\sigma^5 - \frac{\alpha\sigma^2}{\bar{v}\sqrt{t}} - 4(\gamma-1)\bar{v}\sqrt{t}t\sigma^3\bar{\eta}'(t)\tilde{\varphi}(\sigma,n,v,t,\varepsilon)\right),\\
\frac{\mathrm{d}\bar{v}}{\mathrm{d}\bar{z}} &= \frac{3}{4\bar{\eta}(t)}\left(\bar{v}\sigma^4 + \frac{1}{\gamma\bar{v}} - \frac{1}{\gamma-1}\frac{n}{\sqrt{t}}\right) - 2\varepsilon\bar{v}\sigma^3 - \frac{\sigma^2\bar{v}}{2t}\tilde{\varphi}(\sigma,n,v,t,\varepsilon),\\
\frac{\mathrm{d}t}{\mathrm{d}\bar{z}} &= \frac{\theta\sigma^2}{\bar{\zeta}(t)}\left(\bar{v}\sigma^2n\sqrt{t} - \frac{\gamma-1}{2}\bar{v}^2t\sigma^6 - \alpha\sigma^3 + \frac{1}{\gamma}t\sigma^2 - \sigma^2 + 4\varepsilon(\gamma-1)\bar{\eta}(t)\bar{v}^2t\sigma^5\right),
\end{aligned} \tag{4.8}$$

which is equivalent to (4.7) for $\sigma > 0$ (though we note that the transformation itself extends smoothly to the region $\sigma < 0$). We now analyze (4.8) for $0 \le \sigma < \sigma_0$ for some small $\sigma_0 > 0$. We first observe that this system has a surface of fixed points in the subspace $\sigma = 0$, defined via the relation

$$\frac{1}{\gamma\bar{v}} = \frac{1}{\gamma-1}\frac{n}{\sqrt{t}}. \tag{4.9}$$

In other words, for each fixed t, n, there exists a fixed point when $\sigma = 0$ where $\bar{v}$ is defined by (4.9). Linearization around any such fixed point reveals a triple zero eigenvalue, and a single negative eigenvalue $-\frac{\gamma}{(\gamma-1)^2}\frac{n^2}{t}$, with corresponding eigenvector aligned in the $\bar{v}$-direction. This surface of fixed points therefore forms part of a three-dimensional center manifold $\mathcal{W}^{\mathrm{c}}_{\infty}$ at infinity ($\sigma = 0$) with one-dimensional stable fibers, which extends into the region $\sigma < \sigma_0$ for $\sigma_0 \ll 1$; see Figure 5. We now examine the flow on this center manifold.

The center manifold $\mathcal{W}^{\mathrm{c}}_{\infty}$ can be expressed as a graph over the center subspace, that is, $\bar{v} = \frac{\gamma-1}{\gamma}\frac{\sqrt{t}}{n} + \mathcal{O}(\sigma)$, and the flow on the center manifold is therefore given by

$$\begin{aligned}
\frac{\mathrm{d}\sigma}{\mathrm{d}\bar{z}} &= -\varepsilon\sigma^4,\\
\frac{\mathrm{d}n}{\mathrm{d}\bar{z}} &= -\varepsilon\sigma^4\left(\frac{\alpha\gamma n}{(\gamma-1)\sqrt{t}} + \mathcal{O}(\sigma)\right),\\
\frac{\mathrm{d}t}{\mathrm{d}\bar{z}} &= \frac{\theta\sigma^4}{\bar{\zeta}(t)}\left(t - 1 + \mathcal{O}(\sigma)\right).
\end{aligned} \tag{4.10}$$

Performing another rescaling $\mathrm{d}\tilde{z} = \sigma^2\mathrm{d}z$ results in the system

$$\begin{aligned}
\frac{\mathrm{d}\sigma}{\mathrm{d}\tilde{z}} &= -\varepsilon,\\
\frac{\mathrm{d}n}{\mathrm{d}\tilde{z}} &= -\varepsilon\left(\frac{\alpha\gamma n}{(\gamma-1)\sqrt{t}} + \mathcal{O}(\sigma)\right),\\
\frac{\mathrm{d}t}{\mathrm{d}\tilde{z}} &= \frac{\theta}{\bar{\zeta}(t)}\left(t - 1 + \mathcal{O}(\sigma)\right),
\end{aligned} \tag{4.11}$$

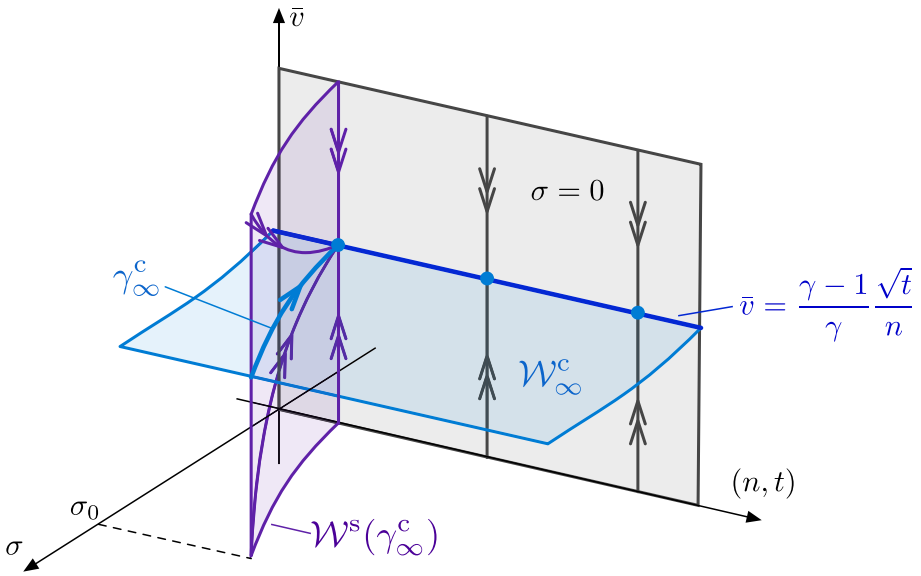

Figure 5. *Shown are the dynamics of (4.8) near $\sigma = 0$. The three-dimensional center manifold $\mathcal{W}_\infty^{\mathrm{c}}$ is foliated by one-dimensional stable fibers (one of the center directions has been suppressed). Also shown are the special trajectory $\gamma_\infty^{\mathrm{c}}$ as well as its stable fiber $\mathcal{W}^{\mathrm{s}}(\gamma_\infty^{\mathrm{c}})$.*

which is a slow-fast system with singular perturbation parameter ε and again equivalent to (4.7) for $\sigma > 0$, extending smoothly to $\sigma < 0$. This system has a two-dimensional normally repelling critical manifold $\mathcal{C}_0$ given by the set of equilibria of (4.11) when $\varepsilon = 0$. Therefore $\mathcal{C}_0$ can be expressed as a graph $t = 1 + \mathcal{O}(\sigma)$, and the flow on $\mathcal{C}_0$ is given by the reduced flow

$$\begin{aligned} \frac{\mathrm{d}\sigma}{\mathrm{d}\tilde{y}} &= -1, \\ \frac{\mathrm{d}n}{\mathrm{d}\tilde{y}} &= -\left(\frac{\alpha\gamma n}{(\gamma - 1)} + \mathcal{O}(\sigma)\right), \end{aligned} \tag{4.12}$$

on the slow timescale $\tilde{y} = \varepsilon\tilde{z}$. The flow off of $\mathcal{C}_0$ is governed by expansion along one-dimensional fast unstable fibers. We have the following.

Lemma 4.2. *For each $n_\infty, t_\infty > 0$ and sufficiently small σ_0, there exists $\varepsilon_0 > 0$ such that for $\varepsilon \in (0, \varepsilon_0)$, there exists $\tilde{z}_\infty, n_0, t_0 > 0$ and a solution $(\sigma, n, t)(\tilde{z})$ to (4.11) satisfying $(\sigma, n, t)(0) = (\sigma_0, n_0, t_0)$ and $(\sigma, n, t)(\tilde{z}_\infty) = (0, n_\infty, t_\infty)$ with*

$$n_0 = n_\infty + \mathcal{O}(\sigma_0, \varepsilon), \qquad t_0 = 1 + \mathcal{O}(\sigma_0, \varepsilon). \tag{4.13}$$

Proof. This result follows from standard methods of geometric singular perturbation theory. The critical manifold $\mathcal{C}_0$ perturbs for small $\varepsilon > 0$ to a normally hyperbolic slow manifold $\mathcal{C}_\varepsilon$ which is $\mathcal{O}(\varepsilon)$-close to $\mathcal{C}_0$, and the flow on this manifold is an $\mathcal{O}(\varepsilon)$-perturbation of the reduced flow (4.12). Furthermore, the unstable fibers of $\mathcal{C}_0$, given by curves aligned in the t-direction, perturb to form the unstable foliation of the slow manifold $\mathcal{C}_\varepsilon$. The perturbed flow is then given by the slow flow on $\mathcal{C}_\varepsilon$ along with exponential expansion along the fibers; see Figure 6.

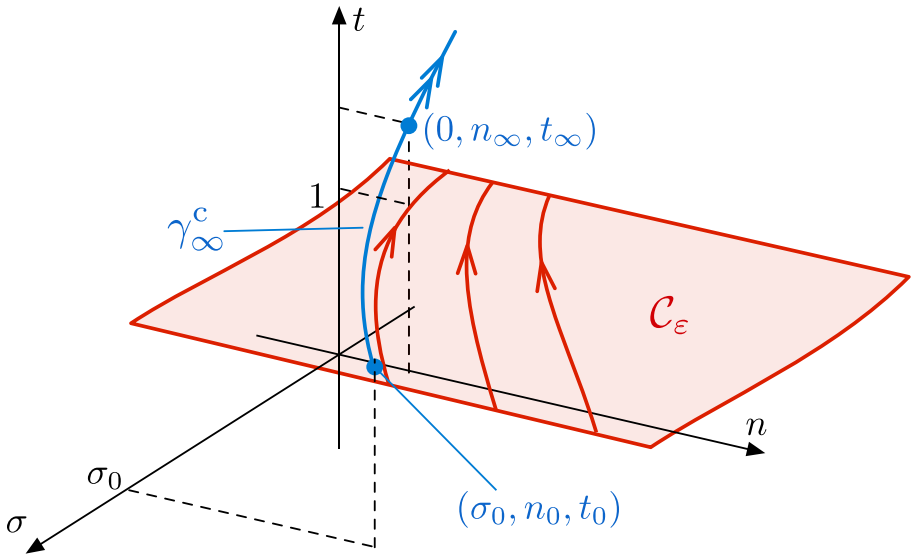

Figure 6. *Shown is the flow given by (4.11) on the three-dimensional center manifold $\mathcal{W}^c_\infty$ near $\sigma = 0$. The trajectory γ^c_∞ from Lemma 4.2 which satisfies the appropriate boundary conditions lies on one of the unstable fibers of the slow manifold $\mathcal{C}_\varepsilon$.*

We choose the fiber of $\mathcal{C}_\varepsilon$ which intersects the set $\{\sigma = 0, n = n_\infty\}$ at $t = t_\infty$. This solution is then evolved under the reverse flow of (4.11), until reaching $\sigma = \sigma_0$, which occurs after time $\sigma_0/\varepsilon =: \tilde{z}_\infty$. In backward time, the t coordinate is contracted exponentially close to the slow manifold $\mathcal{C}_\varepsilon$, so that $t = 1 + \mathcal{O}(\sigma_0, \varepsilon) := t_0$, while the n-coordinate changes by at most an $\mathcal{O}(\sigma_0, \varepsilon)$ amount, so that $n = n_\infty + \mathcal{O}(\sigma_0, \varepsilon) =: n_0$. The coordinates (σ_0, n_0, t_0) therefore define an initial condition which reaches $(\sigma, n, t) = (0, n_\infty, t_\infty)$ after time $\tilde{z}_\infty$, which completes the proof. ∎

Lemma 4.2 guarantees the existence of a solution, which we call γ^c_∞, on the far field center manifold $\mathcal{W}^c_\infty$ which is asymptotic to $(n, t) = (n_\infty, t_\infty)$ as $\sigma \to 0$, or equivalently as $s \to \infty$; see Figure 6. In the full space, we now select the stable fiber of the solution γ^c_∞, which defines a two-dimensional manifold $\mathcal{W}^s(\gamma^c_\infty)$, as shown in Figure 5. We claim that this manifold serves as a boundary manifold which transversely intersects $\mathcal{W}^u(\mathcal{S}^{sub}_0)$ in the subspace $s = s_1$ as in the proof of Proposition 3.6. This is the content of the following proposition.

Proposition 4.3. *For each $n_\infty, t_\infty > 0$, and each sufficiently small $\sigma_0 > 0$, there exists $\varepsilon_0 > 0$ such that for all $\varepsilon \in (0, \varepsilon_0)$, the manifold $\mathcal{W}^s(\gamma^c_\infty)$ transversely intersects $\mathcal{W}^u(\mathcal{S}^{sub}_0)$ in the subspace $s = 1/\sigma_0$.*

Proof. We consider the intersection of $\mathcal{W}^s(\gamma^c_\infty)$ with the set $s = 1/\sigma_0 =: s_1$, or equivalently $\sigma = \sigma_0$. By Lemma 4.2 that the basepoint of this fiber on the center manifold $\mathcal{W}^c_\infty$ satisfies $(n, t) = (n_0, t_0) = (n_\infty, t_\infty) + \mathcal{O}(\sigma_0, \varepsilon)$, and the fiber itself is aligned along the strong stable subspace normal to $\mathcal{W}^c_\infty$.

We now determine how the manifold $\mathcal{W}^u(\mathcal{S}^{sub}_0)$ behaves near the subspace $s = s_1$. We recall that the fast system (3.2) can be equivalently reformulated in terms of the variable $\sigma = 1/s$ as the system (4.8), and the saddle slow manifold $\mathcal{S}^{sub}_0$ could instead be constructed

as an invariant manifold using these equations—and we note that any two constructions of the perturbation of a normally hyperbolic critical manifold may differ only by exponentially small quantities. We observe that when $\sigma = \sigma_0, \varepsilon = 0$ (and noting that v satisfies $v < 1$ on the saddle branch and is in particular bounded uniformly for large s) we obtain the singular fast system

$$\begin{aligned} \frac{\mathrm{d}\bar{v}}{\mathrm{d}\bar{z}} &= \frac{3}{4\bar{\eta}(t)}\left(\bar{v}\sigma_0^4 + \frac{1}{\gamma\bar{v}} - \frac{1}{\gamma-1}\frac{n}{\sqrt{t}}\right) - \frac{\sigma_0^2\bar{v}}{2t}\tilde{\varphi}(\sigma_0, n, v, t, 0), \\ \frac{\mathrm{d}t}{\mathrm{d}\bar{z}} &= \frac{\theta\sigma_0^2}{\bar{\zeta}(t)}\left(\bar{v}\sigma_0^2 n\sqrt{t} - \frac{\gamma-1}{2}\bar{v}^2 t\sigma_0^6 - \alpha\sigma_0^3 + \frac{1}{\gamma}t\sigma_0^2 - \sigma_0^2\right), \end{aligned} \tag{4.14}$$

from which we obtain the subsonic saddle branch $\mathcal{S}_0^{\mathrm{sub}}$ of the critical manifold as the set of fixed points of this system, expressed as the graph

$$\begin{aligned} v &= \frac{\gamma-1}{\gamma n} + \mathcal{O}(\sigma_0), \\ t &= 1 + \mathcal{O}(\sigma_0). \end{aligned} \tag{4.15}$$

The linearization of (4.14) about any such fixed point admits one positive and one negative eigenvalue

$$\lambda_0^- := -\frac{3\gamma n^2}{4(\gamma-1)^2} + \mathcal{O}(\sigma_0), \qquad \lambda_0^+ := \theta\sigma_0^4 + \mathcal{O}(\sigma_0^5), \tag{4.16}$$

with corresponding eigenvectors

$$\psi_0^- = \begin{pmatrix} 1 \\ 0 \end{pmatrix} + \mathcal{O}(\sigma_0), \qquad \psi_0^+ = \begin{pmatrix} 1 \\ \frac{2\gamma n}{\gamma-1} \end{pmatrix} + \mathcal{O}(\sigma_0), \tag{4.17}$$

so that the stable manifold of a fixed point on the subsonic saddle branch $\mathcal{S}_0^{\mathrm{sub}}$ of the critical manifold is aligned with the $\bar{v}$-direction in these rescaled coordinates. We recall that the far-field center manifold $\mathcal{W}_\infty^{\mathrm{c}}$ has one-dimensional stable fibers which for $\sigma = 0$ are aligned along the $\bar{v}$-direction. For small $\sigma_0 > 0$, the stable fibers of the center manifold $\mathcal{W}_\infty^{\mathrm{c}}$ are therefore aligned within $\mathcal{O}(\sigma_0)$ of ψ_0^- in the subspace $\sigma = \sigma_0$ and hence are aligned with the stable fibers of $\mathcal{S}_0^{\mathrm{sub}}$ to leading order in σ_0. Since the stable fibers of $\mathcal{S}_0^{\mathrm{sub}}$ transversely intersect its unstable manifold $\mathcal{W}^{\mathrm{u}}(\mathcal{S}_0^{\mathrm{sub}})$, with fibers aligned in the ψ_0^+-direction, we have that $\mathcal{W}^{\mathrm{s}}(\gamma_\infty^{\mathrm{c}})$ transversely intersects $\mathcal{W}^{\mathrm{u}}(\mathcal{S}_0^{\mathrm{sub}})$ in the subspace $\sigma = \sigma_0$, which completes the proof. ∎

4.4. Accelerating versus decelerating stellar winds. While the construction of transonic stellar wind solutions in sections 4.2–4.3 is valid for any value of $1 < \gamma < 5/3$, and such solutions transition from subsonic to supersonic speeds along a canard solution through the sonic point, the physical speed $u = cv$ of such a solution may actually decrease when crossing the sonic point. In the following lemma, we show that for $\gamma \in (1, 3/2)$, the transonic stellar wind accelerates through the sonic point and decelerates for $\gamma \in (3/2, 5/3)$.

Lemma 4.4. *For a transonic solution constructed as in Proposition 3.6, for $\gamma \in (1, 3/2)$ the speed u is increasing through the sonic point while for $\gamma \in (3/2, 5/3)$, u decreases through the sonic point.*

Proof. Using (2.12), along the critical manifold $\mathcal{S}_0$ we compute

$$\begin{aligned} \frac{\mathrm{d}u}{\mathrm{d}s} &= \frac{\mathrm{d}}{\mathrm{d}s}(cv) = \frac{\mathrm{d}}{\mathrm{d}s}\left(\sqrt{\gamma R k_T}\, tv\right) \\ &= \frac{8v\sqrt{\gamma R k_T}}{s^2\left(v^2(\gamma-1)+2\right)}\left(\frac{1-s}{1-v^2} - \frac{(\gamma-1)v}{5-3\gamma}\right), \end{aligned} \tag{4.18}$$

where we used (3.21) and (3.22). By inspecting the eigenvectors of the linearization (3.27) at the folded saddle, we see the canard Φ_0^c approaches the sonic point (3.26) along the line

$$v - 1 = \sqrt{\frac{5-3\gamma}{2}}(s-1). \tag{4.19}$$

Hence we can evaluate (4.18) along the canard Φ_0^c at the sonic point as

$$\left.\frac{\mathrm{d}u}{\mathrm{d}s}\right|_{(s,v)=(1,1)} = \frac{4\sqrt{2\gamma R k_T}}{(\gamma+1)(5-3\gamma)}\left(\sqrt{5-3\gamma} - \sqrt{2}(\gamma-1)\right). \tag{4.20}$$

We see that this expression is positive (so that the transonic canard accelerates through the sonic point) whenever $1 < \gamma < \gamma^*$, where γ^* is the unique positive solution of the equation

$$\sqrt{5-3\gamma} - \sqrt{2}(\gamma-1) = 0, \tag{4.21}$$

which can be solved directly to find $\gamma^* = 3/2$. ∎

4.5. Proof of Theorem 2.1. In this section, we briefly conclude the proof of the main result, Theorem 2.1.

Proof of Theorem 2.1. Consider (2.10). Fix $\gamma \in (1, 5/3)$ and let the Prandtl number $\theta > 0$ be sufficiently small. Fix an asymptotic pressure, $p_\infty \in (0, \infty)$, and asymptotic temperature, $T_\infty \in (0, \infty)$ as $r \to \infty$. Also let r_0, the radius of the star, satisfy

$$r_0 < r_{\mathrm{sp}} := \frac{4E(\gamma-1)}{GM(5-3\gamma)}.$$

The value r_{sp} corresponds to the radius of the sonic point; hence case $r_0 > r_{\mathrm{sp}}$ corresponds to the radius of the star being greater than the radius of the sonic point, which obstructs the existence of a transonic canard trajectory originating at the stellar surface, and only fully subsonic solutions are possible.

In Proposition 3.6, it was shown that the right-hand boundary condition at $s = s_1$ determines whether a subsonic or a transonic solution is selected in (3.2): given the critical faux canard value $v = v_1^f$ and the chosen boundary condition $v = v_1^b$, if $0 < v_1^b < v_1^f$, then a subsonic trajectory is selected, and in the case where $v_1^f < v_1^b < v_1^c$, a transonic trajectory (with accompanying fast shock) is selected. In order to determine the asymptotic behavior of

these solutions as $r \to \infty$, we see that this depends on the behavior of the faux canard orbit Φ_0^f when s gets large, and in particular the asymptotics of the critical value v_1^f.

The faux canard Φ_0^f lies on the level set $E(s,v) = E_0$, where E, E_0 are given by (3.24) and (3.29), respectively. Keeping this in mind and taking the limit where $s \to \infty$ of (3.24), it is straightforward to see that $v = \mathcal{O}(s^{-2})$ as $s \to \infty$. Therefore, any solution $v(s)$ satisfies

$$v \sim \frac{\bar{v}}{s^2} \tag{4.22}$$

for some $\bar{v} > 0$, and in particular for the faux canard Φ_0^f, we have that

$$v_1^f \sim \frac{\bar{v}_1^f}{s_1^2} \tag{4.23}$$

for some $\bar{v}_1^f$, as the boundary $s = s_1$ is taken asymptotically large. Using (3.24) and (4.23), we compute

$$\ln\left(\bar{v}_1^f\right) = \frac{\gamma+1}{2(\gamma-1)} \ln\left(\frac{2}{5-3\gamma}\right)$$

in the limit $s \to \infty$, and thus we can explicitly solve for v_1^f as

$$\bar{v}_1^f = \left(\frac{2}{5-3\gamma}\right)^{\frac{\gamma+1}{2(\gamma-1)}}. \tag{4.24}$$

Therefore, for a given solution $v = v(s)$ can find an expression for the pressure at infinity, p_∞, by taking the limit of (2.5) as $s \to \infty$, which yields

$$p_\infty = \rho_\infty R T_\infty = \frac{K\sqrt{RT_\infty}}{k_r^2\sqrt{\gamma}\bar{v}}, \tag{4.25}$$

where we've used (2.4), as well as the scalings (2.20), and (4.22). By the discussion above, the solution is subsonic or transonic depending on the relation of $v(s_1)$ and v_1^f, or equivalently, depending on the relation of the asymptotic scalings $\bar{v}$ and $\bar{v}_1^f$. Thus, using (4.24) and (4.25) we can find the critical asymptotic pressure (in terms of the asymptotic density ρ_∞ and temperature T_∞) which determines whether a solution will be subsonic or transonic as

$$p_\infty^2 = \frac{K^2 R T_\infty}{\gamma k_r^4 \left(\bar{v}_1^f\right)^2} = \frac{K^2 R T_\infty}{\gamma k_r^4}\left(\frac{5-3\gamma}{2}\right)^{\frac{\gamma+1}{\gamma-1}} = k_\infty T_\infty, \tag{4.26}$$

where

$$k_\infty := \frac{K^2 R}{\gamma k_r^4}\left(\frac{5-3\gamma}{2}\right)^{\frac{\gamma+1}{\gamma-1}}. \tag{4.27}$$

Therefore, for any given choice of $p_\infty \in (0,\infty)$ and $T_\infty \in (0,\infty)$ satisfying $p_\infty^2 > k_\infty T_\infty$, we can construct boundary manifolds at infinity, as in section 4.3, which when transported back to a finite radius $s = s_1 >$ will correspond to a choice of $\bar{v}_1^b < \bar{v}_1^f$ by (4.26). This directly implies that $v_1^b < v_1^f$ and therefore the corresponding solution, constructed as in Proposition 3.6(i) for sufficiently large Reynolds number $\mathrm{Re} \gg 1$, will be subsonic on the entire domain $s \in (s_0,\infty)$. Converting to the original physical variables, we obtain a pressure $p(r_0) = p_0$ and temperature $T(r_0) = T_0$ at the stellar surface $r = r_0$ that support this solution, and the solution satisfies $(m(r), T(r)) \to (p_\infty, T_\infty)$ as $r \to \infty$. Furthermore the solution is subsonic on the entire domain $r \in (r_0,\infty)$. This completes the proof of (i).

For (ii), fixing a choice of $p_\infty \in (0,\infty)$ and $T_\infty \in (0,\infty)$ satisfying $p_\infty^2 < k_\infty T_\infty$, and arguing as above, we similarly conclude that $\bar{v}_1^b > \bar{v}_1^f$. Additionally, by examining the projection map (3.32), as $v_+ \to \infty$, it is clear that $v \to \sqrt{\frac{\gamma-1}{2\gamma}} =: \bar{v}_1^c$. Therefore, we have that the boundary condition $v = v_1^b$ satisfies $v_1^f < v_1^b < v_1^c$ for large $s = s_1$. Thus, we can conclude that in this case, we can construct a transonic solution and accompanying fast layer shock for this set of conditions by Proposition 3.6(ii), given that the Reynolds number is sufficiently large $\mathrm{Re} \gg 1$. Converting to the original physical variables, we obtain a pressure $p(r_0) = p_0$ and temperature $T(r_0) = T_0$ at the stellar surface $r = r_0$ that support a transonic stellar wind solution satisfying $(m(r), T(r)) \to (p_\infty, T_\infty)$ as $r \to \infty$. The solution is supersonic in the bounded region between the sonic point and the viscous layer shock and is otherwise subsonic. ∎

5. Discussion. In this paper, we constructed steady, spherically symmetric transonic stellar wind solutions in a one-fluid stellar wind model under the effects of heat conduction and viscosity, in the regime of small Reynolds number and small Prandtl number. The solutions were constructed rigorously using geometric singular perturbation techniques; solutions arise as perturbations from singular orbits comprising a saddle canard trajectory, which allows for the transition from subsonic speeds at the stellar surface to supersonic speeds, followed by a fast layer shock to return to subsonic speeds in the far field. These dynamics are characterized by the flow on a two-dimensional critical manifold, with a repelling supersonic branch and saddle-type subsonic branch separated by a fold curve, with a folded singularity, called the sonic point, which organizes the canard dynamics and allows for the transition to supersonic speeds. The location of the shock is then determined by the far-field boundary conditions.

In fact, in the (physically relevant) situation in which the far-field asymptotic pressure and density are small, while the mass flux is large, we obtain leading order estimates on the location of the termination shock. The far-field velocity is determined from the mass flux and asymptotic density via

$$\lim_{r\to\infty} r^2 u = \frac{K}{\rho_\infty}. \tag{5.1}$$

Converting to dimensionless variables, we define

$$\bar{v}_\infty := \lim_{s\to\infty} s^2 v = \frac{K}{k_r^2 c \rho_\infty} = \frac{K\sqrt{RT_\infty}}{k_r^2\sqrt{\gamma}p_\infty}.$$

For small p_∞ (relative to the other physical parameters), the quantity $\bar{v}_\infty$ satisfies $\bar{v}_\infty \gg 1$; this quantity is related to the location of the shock through the reduced flow on the subsonic branch $\mathcal{S}_0^{\text{sub}}$, and in particular it defines the asymptotic value E_∞ of the conserved quantity $E(s,v)$ as $s \to \infty$ as

$$E_\infty \approx \frac{\ln(\bar{v}_\infty)}{2} - \frac{\gamma+1}{4(\gamma-1)} \ln 2. \tag{5.2}$$

Since the flow on the subsonic branch is to leading order confined to level sets of E, to determine the location of the shock, we must determine the value of s along the canard trajectory Φ^c at which the projected canard $\Psi(\Phi^c)$ satisfies $E(s,v) = E_\infty$. Along the canard trajectory, $v \to \infty$ as $s \to \infty$, so that under the projection Ψ, the corresponding projected v-coordinate satisfies $v^2 \approx \frac{\gamma-1}{2\gamma} =: v_{\text{crit}}^2$, using (3.32). Therefore to find the location of the shock, we solve the relation $E(s, v_{\text{crit}}) = E_\infty$ for s, obtaining

$$s_{\text{crit}}^4 \approx \frac{2\gamma}{\gamma-1} \left(\frac{(\gamma+1)^2}{4\gamma} \right)^{\frac{\gamma+1}{\gamma-1}} \bar{v}_\infty^2. \tag{5.3}$$

Converting back to the physical coordinates, we have that the location of the termination shock satisfies

$$r_{\text{crit}}^4 \approx \frac{2\gamma}{\gamma-1} \left(\frac{(\gamma+1)^2}{4\gamma} \right)^{\frac{\gamma+1}{\gamma-1}} \frac{K^2 R T_\infty}{\gamma p_\infty^2}. \tag{5.4}$$

In particular, for the solar wind, we take the values $K \sim 0.9 - 1.8 \times 10^9$ kg $\cdot$ s^{-1}, $T_\infty \sim 0.4 - 1.8 \times 10^5$ K, $p_\infty \sim 212 - 322$ fPa, $R \sim 4124.2$ J $\cdot$ kg^{-1} $\cdot$ K^{-1}, and $\gamma = 1.4$ as representative of possible physical conditions in the heliosheath [8, 19, 29, 30, 31, 32, 35]. This results in a predicted range for the termination shock at $r_{\text{crit}} \sim 66 - 137$ AU, which is in line with Parker's predictions [10, 23, 28]. We remark that Voyager 1 crossed the termination shock at 94 AU, while Voyager 2 crossed at 84 AU.

We note that the solutions as constructed in Theorem 2.1 are locally unique, in the sense that for given boundary conditions (corresponding to boundary manifolds in the proof of Proposition 3.6), there is precisely one choice of canard trajectory and layer shock which will produce a steady solution to the full system. However, we have not aimed to address the temporal stability of this distinguished solution in the full PDE. Numerical simulations in similar models [4] indicate that such transonic canard trajectories are likely to be stable under perturbations sharing the same spherical symmetry. However, we are not aware of rigorous results in this direction. It remains an interesting direction for further research to perform such a stability analysis. A natural first step would be to linearize the PDE under the assumption of spherical symmetry and search for purely radial eigenfunctions using Evans function methods; much is known regarding the stability of viscous shock waves in one (or more) spatial dimensions [18, 41], though not in the present context with spherical symmetry. In the context of transonic flows, in a one-dimensional model of flow through a nozzle, linear stability of an inviscid sub-to-supersonic solution passing through a canard point has been established in [15]. In the particular case of transonic stellar winds, point eigenvalues are

likely to arise associated with both the saddle canard and the layer shock. The full problem, however, allowing perturbations in the angular variables is likely to be a challenging problem. Some analysis in this direction for similar models of stellar wind has been carried out in, for instance, [3, 20, 25].

Last, we remark that the model itself is of course simplified. However, this simple model is able to provide geometric insight into the stellar wind phenomenon while remaining analytically tractable. Natural extensions would incorporate the effects of multiple fluids and relativistic fluid dynamics. Additionally, we have not yet incorporated the plasma physics of stellar wind into the model, which would allow for a variable magnetic field within the gas; this approach, however, would likely prove challenging, as it would extend the state space to a dimension higher than that which is presented here. These considerations will be the focus of future work.

Appendix A. Construction of fast heteroclinic orbits. In order to prove Proposition 3.4, we create a trapping region bounded by the t- and v-nullclines; in the region of interest, the nullclines can be represented as graphs $t = t(s, n, v)$ and properties of the flow across the nullclines can be determined in order to construct the trapping region. This is accomplished through four technical lemmas. The first lemma shows that $\frac{\mathrm{d}v}{\mathrm{d}z} < 0$ along the branch of the t-nullcline which lies between the two fixed points, while the second shows that $\frac{\mathrm{d}t}{\mathrm{d}z} > 0$ along the branch of the v-nullcline between the two fixed points. The final two lemmas are concerned with showing that the v-nullcline lies above the t-nullcline and that the t-nullcline does not have any turning points for $v \in (v_-, v_+)$. This creates a trapping region under the reverse flow of (3.3); see Figure 4.

Lemma A.1. *For all $\gamma \in (1, 5/3)$, and $s, n > 0$ satisfying the bounds as in Lemma 3.2, the branch of the nullcline $f_2(s, n, v, t, 0) = 0$ containing the two fixed points $(v_\pm, t_\pm)$ can be represented as a graph $t = t_2(s, n, v)$, and we have that $f_1(s, n, v, t, 0) < 0$ whenever $t = t_2(s, n, v), v \in (v_-, v_+)$.*

Proof. From (3.1), we notice that $f_2(s, n, v, t, 0)$ is quadratic in $\sqrt{t}$. Thus we can solve $f_2(s, n, v, t, 0) = 0$ for $\sqrt{t}$ and then square the result to obtain

$$t_2^{\pm}(s, n, v) = \left(\frac{-\gamma v n s^3 \pm \sqrt{\gamma^2 v^2 n^2 s^6 + 2s\gamma(\alpha + s)\left(2 - \gamma\left(\gamma - 1\right) v^2\right)}}{s(2 - \gamma(\gamma - 1)v^2)} \right)^2, \tag{A.1}$$

where we note that for $t_2^-(s, n, v)$, this expression is only physically meaningful when $s(2 - \gamma(\gamma - 1)v^2) < 0$. Furthermore, as we only consider positive, real values of t, the discriminant in (A.1) must be positive. We proceed to determine which branch $t_2^{\pm}$ contains the fixed points $(v_\pm, t_\pm)$. We note that any fixed point of (3.3) must also satisfy $f_1(s, n, v, t, 0) = 0$. In the case of $t = t_2^-$, we compute

$$\begin{aligned} f_1\left(s, n, v, t_2^-, 0\right) &= \frac{3}{4\bar{\eta}(t)} \left(\frac{v}{s^2} + \frac{1}{\gamma s^2 v} - \frac{n}{\gamma - 1} \frac{s(\gamma(\gamma - 1)v^2 - 2)}{\gamma v n s^3 + \sqrt{\gamma^2 v^2 n^2 s^6 + 2s\gamma(\alpha + s)\left(2 - \gamma\left(\gamma - 1\right) v^2\right)}} \right) \\ &\geq \frac{3}{4\bar{\eta}(t)} \left(\frac{v}{s^2} + \frac{1}{\gamma s^2 v} - \frac{n}{\gamma - 1} \frac{s(\gamma(\gamma - 1)v^2 - 2)}{\gamma v n s^3} \right) \end{aligned}$$

$$= \frac{3(\gamma+1)}{4\bar{\eta}(t)s^2 v\gamma(\gamma-1)}$$
$$> 0.$$

Thus, on the $t = t_2^-$ branch of the t-nullcline, $f_1(s,n,v,t,0)$ has fixed sign and therefore this branch cannot contain any fixed points.

Hence we restrict attention to the branch $t = t_2^+$, which contains both fixed points. The expression (A.1) appears to be undefined as $v^2 \to \frac{2}{\gamma(\gamma-1)}$. However, using l'Hôpital's rule,

$$\lim_{v^2 \to \sqrt{\frac{2}{\gamma(\gamma-1)}}} t_2^+(s,n,v) = \lim_{v \to \sqrt{\frac{2}{\gamma(\gamma-1)}}} \left(\frac{-\gamma v n s^3 + \sqrt{\gamma^2 v^2 n^2 s^6 + 2s\gamma(\alpha+s)\left(2-\gamma(\gamma-1)v^2\right)}}{s(2-\gamma(\gamma-1)v^2)} \right)^2$$
$$= \frac{\gamma\left(n^2 s^5 + 2(\alpha+s)(\gamma-1)\right)^2}{8(\gamma-1)n^2 s^6}$$

so that the graph $t_2^+(s,n,v)$ is in fact continuous in v.

We now are able to determine the sign of $f_1(s,n,v,t,0)$ on the branch $t_2^+(s,n,v)$ of the t-nullcline between the two fixed points $v = v_\pm$. Since $t_2^+(s,n,v)$ and $f_1(s,n,v,t,0)$ are continuous in v, it suffices to evaluate $f_1(s,n,v,t,0)$ at one point in the interval (v_-, v_+) to determine its sign for all $v \in (v_-, v_+)$. Choose for simplicity $v = 1$. Then we have

(A.2)
$$f_1(s,n,1,t_2^+(s,n,1),0) = \frac{3(\gamma+1)}{4\gamma\bar{\eta}(t)} \left(\frac{1}{s^2} - \frac{(2-\gamma)}{\gamma-1} \frac{\gamma s n}{-\gamma n s^3 + \sqrt{\gamma^2 n^2 s^6 + 2s\gamma(\alpha+s)(2-\gamma)(\gamma+1)}} \right)$$
$$< 0,$$

where we used the bounds on s, n as in Lemma 3.2. ∎

We now prove a similar lemma for the v-nullcline.

Lemma A.2. *For all $\gamma \in (1, 5/3)$, and $s, n > 0$ satisfying the bounds as in Lemma 3.2, the branch of the nullcline $f_1(s,n,v,t,0) = 0$ containing the two fixed points $(v_\pm, t_\pm)$ can be represented as a graph $t = t_1^-(s,n,v)$, and we have that $f_2(s,n,v,t,0) > 0$ whenever $t = t_1^-(s,n,v), v \in (v_-, v_+)$.*

Proof. Setting $f_1(s,n,v,t,0) = 0$ in (3.3), along the v-nullcline, we have that

$$\frac{3}{2\bar{\eta}(t)v} \left(\frac{t}{s^2}\left(v + \frac{1}{\gamma v}\right) - \frac{n\sqrt{t}}{\gamma-1} \right) = \frac{\theta}{\bar{\zeta}(t)} \left(vn\sqrt{t} - \frac{\gamma-1}{2}\frac{v^2 t}{s^2} - \frac{\alpha}{s^3} + \frac{1}{\gamma}\frac{t}{s^2} - \frac{1}{s^2} \right), \tag{A.3}$$

which is a quadratic expression in $\sqrt{t}$, noting that $\bar{\eta}(t) = \bar{\zeta}(t)$ from (2.15). This expression can be solved for two roots $t = t_1^\pm(s,n,v)$ given by

$$t_1^\pm(s,n,v) = \left(\frac{B(s,n,v) \pm \left(B(s,n,v)^2 - 4A(s,n,v)C(s,n,v)\right)^{1/2}}{2A(s,n,v)} \right)^2, \tag{A.4}$$

where

$$A(s,n,v) = \frac{3}{vs^2}\left(v + \frac{1}{\gamma v}\right) + \frac{\theta}{s^2}\left((\gamma-1)v^2 - \frac{2}{\gamma}\right),$$
$$B(s,n,v) = \frac{3n}{2v(\gamma-1)} + \theta v n,$$
$$C(s,n,v) = \theta\frac{(\alpha+s)}{s^3},$$

and for small $0 < \theta \ll 1$ these roots can be expressed as

$$t_1^+(s,n,v) = \frac{\gamma^2 n^2 v^2 s^4}{(\gamma-1)^2(\gamma v^2+1)^2} + \mathcal{O}(\theta),$$
$$t_1^-(s,n,v) = \frac{4\theta^2(\alpha+s)^2 v^2(\gamma-1)^2}{9n^2 s^6} + \mathcal{O}(\theta^3). \tag{A.5}$$

We first consider the branch $t = t_1^-$ and using (A.3), we compute

$$\begin{aligned} f_2(s,n,v,t_1^-,0) &= \frac{3}{2\bar{\eta}(t_1^-)v}\left(\frac{t_1^-}{s^2}\left(v+\frac{1}{\gamma v}\right) - \frac{n\sqrt{t_1^-}}{\gamma-1}\right) \\ &= -\frac{\theta(\alpha+s)}{\bar{\eta}(t_1^-)s^3} + \mathcal{O}(\theta^2) \\ &< 0 \end{aligned} \tag{A.6}$$

for all sufficiently small $\theta > 0$. Since the sign of f_2 is fixed, the branch $t = t_1^-$ contains no fixed points.

We now consider the branch $t = t_1^+$, on which

$$f_2(s,n,v,t_1^+,0) = \frac{3t_1^+}{2\bar{\eta}(t_1^+)v}\left(\frac{1}{s^2}\left(v+\frac{1}{\gamma v}\right) - \frac{n}{(\gamma-1)\sqrt{t_1^+}}\right). \tag{A.7}$$

As in the proof Lemma A.1, we can determine the sign of this expression on the interval (v_-, v_+) by examining its sign when $v = 1$. By a similar computation as in the proof of Lemma A.1, again using the lower bound on n^2 from Lemma 3.2, we obtain

$$f_2(s,n,1,t_1^+(s,n,1),0) < 0. \tag{A.8}$$

■

The next lemma describes the relative positioning of the v- and t-nullclines in the phase portrait of (3.3).

Lemma A.3. *For all $s > 0$, $\gamma \in (1, 5/3)$, $v \in (v_-, v_+)$, and n as bounded in Lemma 3.2, the v-nullcline lies above the t-nullcline.*

Proof. By the proofs of Lemmas A.1 and A.2, the fixed points $(v_\pm, t_\pm)$ are contained on the curves $t = t_2^+(s,n,v)$ and $t = t_1^+(s,n,v)$, which represent branches of the t- and v-nullclines, respectively. We consider the quantity

$$\Delta_{\text{null}}(s,n,v) := \frac{1}{n^2}\left(t_1^+(s,n,v) - t_2^+(s,n,v)\right). \tag{A.9}$$

Since $t = t_2^+(s,n,v)$ and $t = t_1^+(s,n,v)$ are continuous in $v \in (v_-, v_+)$, and $\Delta_{\text{null}} = 0$ only at the two fixed points $v = v_\pm$, it is sufficient to determine the sign of Δ_{null} by evaluating at $v = 1 \in (v_-, v_+)$. Furthermore, we note from (A.1) and (A.4) that the quantity $n^{-2}t_2^+(s,n,v)$ is decreasing in n^2, while $n^{-2}t_1^+(s,n,v)$ is increasing in n^2, so that for a given (s,v), $\Delta_{\text{null}}(s,n,v)$ in minimized by using the lower bound on n^2 from Lemma 3.2, whence we obtain

$$\begin{aligned}\Delta_{\text{null}}(s,n,1) &> \frac{1}{n_{\min}^2}\left(t_1^+(s,n_{\min},1) - t_2^+(s,n_{\min},1)\right)\\ &= 0,\end{aligned}$$

so that the v-nullcline lies above the t-nullcline, as claimed. ∎

Last, we show that the curve $t = t_2^+(s,n,v)$ does not have any turning points on the interval $v \in (v_-, v_+)$, which ensures that flow of (3.3) points out of the region bounded by the nullclines for $v \in (v_-, v_+)$.

Lemma A.4. *For all $s > 1$, $\gamma \in (1, 5/3)$, $v \in (v_-, v_+)$, and n as in Lemma 3.2, we have $\partial_v t_2^+(s,n,v) \neq 0$.*

Proof. Since $(t_2^+(s,n,v))^{1/2} > 0$ for $v \in (v_-, v_+)$, zeros of $\partial_v t_2^+$ correspond to zeros of

$$\frac{\partial}{\partial v}\left(\sqrt{t_2^+}\right) = \frac{1}{2\sqrt{t_2^+}}\frac{\partial t_2^+}{\partial v}. \tag{A.10}$$

Hence we search for zeros of the latter and show that none occur in the interval $v \in (v_-, v_+)$. After a lengthy computation, we find that zeros can only occur when

$$v^2 = v_*^2 := \frac{2n^2 s^5}{\gamma(\gamma-1)\left(2(\alpha+s)(\gamma-1) - n^2 s^5\right)}. \tag{A.11}$$

We now claim that $v_* \notin (v_-, v_+)$, and in particular, $v_*^2 > v_+^2$. Using (3.14) we have that

$$v_+^2 = v_*^2 \frac{\gamma}{2}\left(1 - \frac{2(\alpha+s)(\gamma-1)^2}{\gamma n^2 s^5} + \sqrt{\frac{1}{s} - \frac{2(\alpha+s)(\gamma-1)^2(\gamma+1)}{\gamma^2 n^2 s^6}}\right), \tag{A.12}$$

Since the factor on the right-hand side of (A.12) is increasing in n, using the upper bound $n < n_{\max}$ from the proof of Lemma 3.2, we have that

$$\begin{aligned}v_+^2 &< \frac{v_*^2}{2}\left(1 + \frac{1}{\sqrt{s}}\right)\\ &< v_*^2\end{aligned}$$

when $s > 1$. Therefore we conclude that there are no critical points of the t-nullcline in the interval (v_-, v_+) for all $s > 1$, $\gamma \in (1, 5/3)$, and n as bounded in Lemma 3.2. ∎

Using Lemmas A.1–A.4, we can now complete the proof of Proposition 3.4.

Proof of Proposition 3.4. Fix $s > 1$, and n bounded as in Lemma 3.2. Consider the layer problem (3.3). By Proposition 3.1 and Lemma 3.2, there exists a repelling fixed point (v_+, t_+) of (3.3) on the supersonic branch of the critical manifold, $\mathcal{S}_0^{\text{super}}$, and a saddle fixed point (v_-, t_-) on the subsonic branch $\mathcal{S}_0^{\text{sub}}$.

Both of these fixed points must lie on both the v- and t-nullclines. The results of Lemmas A.1–A.4 guarantee that these two nullclines can be given as graphs $t = t(v)$ for $v \in (v_-, v_+)$ which bound a trapping region (under the reverse flow of (3.3)), such that the flow of (3.3) points out of this region in forward time. Following the stable manifold of the saddle fixed point (v_-, t_-) under the reverse flow of (3.3), we have that this trajectory is confined to the trapping region. Any periodic orbit must intersect the nullclines, hence there are no periodic orbits contained entirely in the trapping region. Therefore, by the Poincaré–Bendixson theorem, this trajectory must approach a fixed point, and hence there exists a heteroclinic orbit from $(v_+,\ t_+)$ to $(v_-,\ t_-)$ for each $s > 1$ and n as bounded in Lemma 3.2. ∎

Appendix B. Center manifold analysis near the sonic point. We shift the sonic point to the origin and perform a linear change of coordinates

$$
\begin{aligned}
\tilde{s} &= s - 1,\\
\tilde{n} &= n - n^*,\\
v_1 &= \frac{-8(\gamma-1)\theta}{(5-3\gamma)(4\theta+3\gamma-3)}(v-1) + \frac{(\gamma-1)(2\theta-3)}{4\theta+3\gamma-3}(t-t^*),\\
v_2 &= \frac{8(\gamma-1)\theta}{(5-3\gamma)(4\theta+3\gamma-3)}(v-1) + \frac{2(1+\gamma)\theta}{4\theta+3\gamma-3}(t-t^*)
\end{aligned}
\tag{B.1}
$$

to diagonalize the fast subsystem at the linear level at the sonic point for $\varepsilon = 0$, resulting in the system

$$
\begin{aligned}
\frac{\mathrm{d}\tilde{s}}{\mathrm{d}z} &= \varepsilon \tilde{g}_1(\tilde{s}, \tilde{n}, v_1, v_2, \varepsilon),\\
\frac{\mathrm{d}\tilde{n}}{\mathrm{d}z} &= \varepsilon \tilde{g}_2(\tilde{s}, \tilde{n}, v_1, v_2, \varepsilon),\\
\frac{\mathrm{d}v_1}{\mathrm{d}z} &= h_1(\tilde{s}, \tilde{n}, v_1, v_2, \varepsilon),\\
\frac{\mathrm{d}v_2}{\mathrm{d}z} &= h_2(\tilde{s}, \tilde{n}, v_1, v_2, \varepsilon),
\end{aligned}
\tag{B.2}
$$

where

$$
\begin{aligned}
\tilde{g}_1(\tilde{s}, \tilde{n}, v_1, v_2, \varepsilon) &:= g_1\left(1+\tilde{s}, n^*+\tilde{n}, 1+V^\dagger(v_1, v_2), t^* + T^\dagger(v_1, v_2), \varepsilon\right),\\
\tilde{g}_2(\tilde{s}, \tilde{n}, v_1, v_2, \varepsilon) &:= g_2\left(1+\tilde{s}, n^*+\tilde{n}, 1+V^\dagger(v_1, v_2), t^* + T^\dagger(v_1, v_2), \varepsilon\right),\\
h_1(\tilde{s}, \tilde{n}, v_1, v_2, \varepsilon) &:= \frac{-8(\gamma-1)\theta}{\bar{\eta}(t)(5-3\gamma)(4\theta+3\gamma-3)} f_1\left(1+\tilde{s}, n^*+\tilde{n}, 1+V^\dagger(v_1, v_2), t^* + T^\dagger(v_1, v_2), \varepsilon\right)\\
&\quad + \frac{(\gamma-1)(2\theta-3)}{\bar{\zeta}(t)(4\theta+3\gamma-3)} f_2\left(1+\tilde{s}, n^*+\tilde{n}, 1+V^\dagger(v_1, v_2), t^* + T^\dagger(v_1, v_2), \varepsilon\right),
\end{aligned}
$$

$$h_2(\tilde{s},\tilde{n},v_1,v_2,\varepsilon) := \frac{8(\gamma-1)\theta}{\bar{\eta}(t)(5-3\gamma)(4\theta+3\gamma-3)} f_1\left(1+\tilde{s}, n^*+\tilde{n}, 1+V^\dagger(v_1,v_2), t^*+T^\dagger(v_1,v_2),\varepsilon\right) + \frac{2(1+\gamma)\theta}{\bar{\zeta}(t)(4\theta+3\gamma-3)} f_2\left(1+\tilde{s}, n^*+\tilde{n}, 1+V^\dagger(v_1,v_2), t^*+T^\dagger(v_1,v_2),\varepsilon\right),$$

and

$$V^\dagger(v_1,v_2) := \frac{-(\gamma+1)(5-3\gamma)}{4(\gamma-1)} v_1 - \frac{(5-3\gamma)(2\theta-3)}{8\theta} v_2,$$
$$T^\dagger(v_1,v_2) := v_1+v_2.$$

The functions h_1, h_2 satisfy

$$h_1(\tilde{s},\tilde{n},v_1,v_2,\varepsilon) = \mathcal{O}(\tilde{s},\tilde{n},v_1^2,v_2^2,\varepsilon),$$
$$h_2(\tilde{s},\tilde{n},v_1,v_2,\varepsilon) = \lambda_+\tilde{v}_2 + \mathcal{O}(\tilde{s},\tilde{n},v_1^2,v_2^2,\varepsilon),$$

where $\lambda_+ > 0$ is given by (4.3), so at the linear level, the dynamics on the center manifold are parameterized by $(\tilde{s},\tilde{n},v_1)$, and the fast unstable dynamics off of the center manifold are governed by the flow in the v_2-direction. By standard results of center manifold theory, there exists a three-dimensional center manifold $\mathcal{W}^{\mathrm{c}}_{\mathrm{sp}}$ which can be represented as a graph $v_2 = V^{\mathrm{c}}_{\mathrm{sp}}(\tilde{s},\tilde{n},v_1,\varepsilon)$ over the center subspace. Changing coordinates via $\tilde{v}_2 = v_2 - V^{\mathrm{c}}_{\mathrm{sp}}(\tilde{s},\tilde{n},v_1,\varepsilon)$, and applying one further coordinate transformation to straighten the strong unstable fibers, so that the flow in the $(\tilde{s},\tilde{n},v_1)$-coordinates is decoupled from v_2, we obtain the system

$$\begin{aligned}
\frac{\mathrm{d}\tilde{s}}{\mathrm{d}z} &= \varepsilon\tilde{g}_1^{\mathrm{c}}(\tilde{s},\tilde{n},v_1,\varepsilon),\\
\frac{\mathrm{d}\tilde{n}}{\mathrm{d}z} &= \varepsilon\tilde{g}_2^{\mathrm{c}}(\tilde{s},\tilde{n},v_1,\varepsilon),\\
\frac{\mathrm{d}v_1}{\mathrm{d}z} &= \tilde{h}_1^{\mathrm{c}}(\tilde{s},\tilde{n},v_1,\varepsilon),\\
\frac{\mathrm{d}\tilde{v}_2}{\mathrm{d}z} &= \tilde{h}_2^{\mathrm{c}}(\tilde{s},\tilde{n},v_1,\tilde{v}_2,\varepsilon),
\end{aligned} \tag{B.3}$$

where

$$\tilde{h}_2^{\mathrm{c}}(\tilde{s},\tilde{n},\tilde{v}_1,\tilde{v}_2,\varepsilon) = \left(\lambda_+ + \mathcal{O}(\tilde{s},\tilde{n},\tilde{v}_1,\tilde{v}_2,\varepsilon)\right)\tilde{v}_2. \tag{B.4}$$

We now complete the proof of Proposition 4.1.

Proof of Proposition 4.1. The dynamics on the center manifold $\mathcal{W}^{\mathrm{c}}_{\mathrm{sp}}$ are governed by the first three equations of (B.3) in the variables $(\tilde{s},\tilde{n},v_1)$. This system is a 2-slow-1-fast singularly perturbed dynamical system with slow variables $(\tilde{s},\tilde{n})$ and fast variable v_1, with perturbation parameter ε, which is in the normal form for a folded saddle canard point in the sense of [37]. In particular, one can verify that the conditions (6)–(7) from [37] hold via applying the linear coordinate transformations (B.1), Taylor expanding in $(\tilde{s},\tilde{n},v_1,v_2)$, and computing the relevant quantities

$$\begin{aligned}
\tilde{h}_1^{\mathrm{c}}(0,0,0,0) &= 0,\\
\frac{\partial \tilde{h}_1^{\mathrm{c}}}{\partial v_1}(0,0,0,0) &= 0,\\
\frac{\partial \tilde{h}_1^{\mathrm{c}}}{\partial \tilde{n}}(0,0,0,0) &= \frac{3\theta\gamma(5-3\gamma)^2}{4(4\theta+3\gamma-3)} \neq 0,\\
\frac{\partial^2 \tilde{h}_1^{\mathrm{c}}}{\partial v_1^2}(0,0,0,0) &= -\frac{3\theta(1+\gamma)(5-3\gamma)^{7/2}}{8\sqrt{2}(\gamma-1)(4\theta+3\gamma-3)} \neq 0,
\end{aligned}$$

where the last two quantities were calculated using Mathematica. Thus within the center manifold $\mathcal{W}^{\mathrm{c}}_{\mathrm{sp}}$, the results of [37] hold, and the assertions of the proposition follow from [37, Theorem 4.1]. ∎

REFERENCES

[1] W. Axford and R. Newman, *Viscous-transonic flow in the accretion and stellar-wind problems*, Astrophys. J., 147 (1967), pp. 230–234, https://doi.org/10.1086/148994.

[2] W. I. Axford, A. J. Dessler, and B. Gottlieb, *Termination of solar wind and solar magnetic field*, Astrophys. J., 137 (1963), pp. 1268–1278, https://doi.org/10.1086/147602.

[3] R. Carovillano and J. King, *Dynamical stability and boundary perturbations of the solar wind*, Astrophys. J., 145 (1966), pp. 426–444.

[4] P. Carter, E. Knobloch, and M. Wechselberger, *Transonic canards and stellar wind*, Nonlinearity, 30 (2017), pp. 1006–1033, https://doi.org/10.1088/1361-6544/aa5743.

[5] S. Chapman, *The viscosity and thermal conductivity of a completely ionized gas*, Astrophys. J., 120 (1954), pp. 151–155, https://doi.org/10.1086/145890.

[6] E. Dahlberg, *On the stellar-wind equations*, Astrophys. J., 140 (1964), pp. 268–275, https://doi.org/10.1086/147913.

[7] E. Dahlberg, *Viscous model of solar wind flow*, J. Geophys. Res. (1896-1977), 75 (1970), pp. 6312–6317, https://doi.org/10.1029/JA075i031p06312.

[8] S. A. Fuselier and I. H. Cairns, *Plasma properties at the Voyager* 1 *crossing of the heliopause*, J. Phys. Conf. Ser., 642, (2015).

[9] C. R. Hasan, B. Krauskopf, and H. M. Osinga, *Saddle slow manifolds and canard orbits in* $\mathbb{R}^4$ *and application to the full Hodgkin–Huxley model*, J. Math. Neurosci., 8 (2018), 5.

[10] T. E. Holzer, *Interaction between the solar wind and the interstellar medium*, Annu. Rev. Astronom. Astrophys., 27 (1989), pp. 199–234.

[11] T. E. Holzer and W. I. Axford, *The theory of stellar winds and related flows*, Annu. Rev. Astronom. Astrophys., 8 (1970), pp. 31–60, https://doi.org/10.1146/annurev.aa.08.090170.000335.

[12] T. E. Holzer, E. Leer, and X.-P. Zhao, *Viscosity in the solar wind*, J. Geophys. Res. Space Phys., 91 (1986), pp. 4126–4132.

[13] J. Hong, C. Yen, and B. Huang, *Characterization of the transonic stationary solutions of the hydrodynamic escape problem*, SIAM J. Appl. Math., 74 (2014), pp. 1709–1741, https://doi.org/10.1137/130919957.

[14] J. M. Hong, C.-H. Hsu, and B.-C. Huang, *Existence and uniqueness of generalized stationary waves for viscous gas flow through a nozzle with discontinuous cross section*, J. Differential Equations, 253 (2012), pp. 1088–1110.

[15] J. M. Hong, C.-H. Hsu, Y.-C. Lin, and W. Liu, *Linear stability of the sub-to-super inviscid transonic stationary wave for gas flow in a nozzle of varying area*, J. Differential Equations, 254 (2013), pp. 1957–1976.

[16] J. M. Hong, C.-H. Hsu, and W. Liu, *Inviscid and viscous stationary waves of gas flow through contracting–expanding nozzles*, J. Differential Equations, 248 (2010), pp. 50–76.

[17] J. M. Hong, C.-H. Hsu, and W. Liu, *Viscous standing asymptotic states of isentropic compressible flows through a nozzle*, Arch. Ration. Mech. Anal., 196 (2010), pp. 575–597.
[18] J. Humpherys, G. Lyng, and K. Zumbrun, *Multidimensional stability of large-amplitude Navier–Stokes shocks*, Arch. Ration. Mech. Anal., 226 (2017), pp. 923–973.
[19] C. Jacobs and S. Poedts, *A polytropic model for the solar wind*, Adv. Space Research, 48 (2011), pp. 1958–1966.
[20] K. Jockers, *On the stability of the solar wind*, Solar Phys., 3 (1968), pp. 603–610.
[21] R. Johnson, *On the continuum theory of the one-fluid solar wind for small Prandtl number*, Proc. A, 348 (1976), pp. 129–142.
[22] C. Jones, *Tracking invariant manifolds up to exponentially small errors*, SIAM J. Math. Anal., 27 (1996), pp. 558–577, https://doi.org/10.1137/S003614109325966X.
[23] M. A. Lee, *The termination shock of the solar wind*, Space Sci. Rev., 78 (1996), pp. 109–116.
[24] X. Lin and M. Wechselberger, *Transonic evaporation waves in a spherically symmetric nozzle*, SIAM J. Math. Anal., 46 (2014), pp. 1472–1504.
[25] Y.-Q. Lou, *Three-dimensional steady compressible perturbations in the magnetohydrodynamic solar wind*, J. Geophys. Res. Space Phys., 98 (1993), pp. 11501–11512.
[26] L. Noble and F. Scarf, *Conductive heating of the solar wind.* I, Astrophys. J., 138 (1963), pp. 1169–1181.
[27] E. N. Parker, *Dynamics of the interplanetary gas and magnetic fields*, Astrophys. J., 128 (1958), pp. 664–676.
[28] E. N. Parker, *Interplanetary Dynamical Processes*, Interscience, New York, 1963.
[29] J. S. Rankin, D. J. McComas, J. D. Richardson, and N. A. Schwadron, *Heliosheath properties measured from a Voyager* 2 *to Voyager* 1 *transient*, Astrophys. J., 883 (2019), 101.
[30] J. Richardson, *Plasma temperature distributions in the heliosheath*, Geophys. Res. Lett., 35 (2008).
[31] J. D. Richardson, *Voyager observations of the interaction of the heliosphere with the interstellar medium*, J. Adv. Res., 4 (2013), pp. 229–233.
[32] J. D. Richardson, J. W. Belcher, P. Garcia-Galindo, and L. F. Burlaga, *Voyager* 2 *plasma observations of the heliopause and interstellar medium*, Nature Astronomy, 3 (2019), pp. 1019–1023.
[33] C. T. Russell, *The solar wind interaction with the earth's magnetosphere: A tutorial*, IEEE Trans. Plasma Sci., 28 (2000), pp. 1818–1830, https://doi.org/10.1109/27.902211.
[34] F. Scarf and L. Noble, *Conductive heating of the solar wind.* II. *the inner corona*, Astrophys. J., 141 (1965), pp. 1479–1491.
[35] W.-W. Shen, *Ratio of specific heats in the solar-wind plasma flow through the earth's bow shock*, J. Geophys. Res., 76 (1971), pp. 8181–8188.
[36] D. Summers, *On the effects of viscosity in one-fluid solar wind theory*, Proc. A, 349 (1976), pp. 53–62.
[37] P. Szmolyan and M. Wechselberger, *Canards in* $\mathbb{R}^3$, J. Differential Equations, 177 (2001), pp. 419–453, https://doi.org/10.1006/jdeq.2001.4001.
[38] T. R. Waters and D. Proga, *Parker winds revisited: An extension to disc winds*, Monthly Notices of the Royal Astronomical Society, 426 (2012), pp. 2239–2265.
[39] M. Wechselberger, *A propos de canards (apropos canards)*, Trans. Amer. Math. Soc., 364 (2012), pp. 3289–3309.
[40] Y. Whang, C. Liu, and C. Chang, *A viscous model of the solar wind*, Astrophys. J., 145 (1966), p. 255.
[41] K. Zumbrun and P. Howard, *Pointwise semigroup methods and stability of viscous shock waves*, Indiana Univ. Math. J., 47 (1998), pp. 741–872.